Advances in elliptical-core two-mode optical fiber sensors

by

Mark S. Miller

Thesis submitted to the Faculty of the
Virginia Polytechnic Institute and State University
in partial fulfillment of the requirements for the degree of
Masters of Science
in
Electrical Engineering

APPROVED:

Richard O. Claus

Richard O. Claus

Ronald J. Pieper

Ronald J. Pieper

Ting-Chung Poon

Ting-Chung Poon

April, 1990

Blacksburg, Virginia

Advances in elliptical-core two-mode optical fiber sensors

by

Mark S. Miller

Richard O. Claus, Chairman

Electrical Engineering

(ABSTRACT)

Methods designed to improve the practicality of the elliptical-core two-mode optical fiber sensors for use in real-life applications are presented. The improvements include the development of insensitive lead fibers and an optical device which allows fringe counting at the output of the sensor. The insensitive leads eliminate extraneous perturbations and effectively isolate the sensing region. The fringe counting optics are designed to generate quadrature-phase shifted signals, thereby allowing the determination of whether the strain is increasing or decreasing.

Work performed to advance the understanding of the effect of sensor placement within a composite specimen is also presented. Optical fiber sensors are embedded between different laminae of a graphite-epoxy composite panel, and the outputs of the sensors are shown to be proportional to the distance of the sensor from the neutral axis.

Acknowledgments

I would like to thank my advisor, Dr. Richard O. Claus, for all of his help and guidance for the past two and a half years. I would also like to thank Dr. Ronald J. Pieper and Dr. Ting Chung Poon for serving on my committee.

I would especially like to thank Kent A. Murphy and Ashish M. Vengsarkar for their long hours of work and help, without which this thesis would never have happened. Thank you also to FEORC for a fun two and a half years.

I am most grateful for the love and support given to me by my family, especially my parents Theodore L. Miller and Martha R. Miller. A most heartfelt thank you goes to my wife, Rebecca, for her love, understanding, and most of all patience during my time in graduate school. Without her support, I do not know if I would have survived this long.

This work was sponsored in part by Poly-Scientific Division, Litton Industries with contract monitor Dr. Norris E. Lewis and by the Virginia Center for Innovative Technology.

Table of Contents

List of Illustrations

List of Tables

1.0 Introduction

The phrase "smart structures" has become well known in recent years[1,2,3]. Smart structures require the development of sensors, actuators and a degree of intelligence within the structure. In other words, the smart structure would be able to determine its condition. Ideally, the final result would be a structure that would act similarly to the human body. Essentially, there would be a "nervous system" to detect the state of the structure and the means to respond. The "nervous system" would be made of many sensors designed to detect specific parameters of the structure so that the "health" of the structure could be determined at any time. With the emergence of optical fiber sensors, the possibility of such a "nervous system" for structures and skins has grown greatly[1,2,3]. Optical fibers are light weight, small, and inexpensive. Optical fibers can also be embedded in many advanced composite materials[4,5], which are becoming the material of choice for many high performance structural applications requiring high strength-to-weight ratios[6]. Embedding fiber sensors in

such materials allows evaluation of the material in a nondestructive mode. The sensors will experience nearly the same effects as the material and evaluation of the material can be done continuously. This method is nondestructive because the material remains intact while the sensing is performed. No cutting or breakage need occur to determine the effects of perturbations.

The major material parameters of interest include strain, temperature, and structural vibrations. An excellent optical fiber sensor for the measurement of strain and vibration is the modal domain sensor[7,8]. This sensor is designed to use the interference between the lowest order modes of the fiber to determine changes in strain. The changes in strain can be either static or dynamic. As optical fiber technology has advanced, the sophistication of this sensor has also advanced. At first, circular-core fiber was the only fiber available but it led to instability problems[9]. With the development of elliptical-core (e-core) fiber, these instabilities effectively are removed[10]. Most current efforts involving modal domain sensors are two-mode sensors; they use only the two lowest order modes in the fiber.

A major problem associated with most sensors is their transformation from a laboratory environment to a practical, real-life application. The two-mode elliptical-core sensor has had these types of problems in its practical implementation. This thesis will address the following issues related to such implementation.

1. Sensitivity of the lead fibers: those fibers leading to and from the active region. If the lead fibers are sensitive to strain or vibration, the sensor may detect perturbations outside of the sensing region which will cause error in the interpretation of the output of the sensor.

2. Fringe counting: the use of fringe counting for the detection of vibrations has been hampered in the past because of the difficulty in determining the change from increasing strain to decreasing strain whenever there is a vibration. If fringe counting is employed, the electronics may miss this change in sign of the strain and give erroneous readings.

This thesis will present techniques designed to overcome these two problems, specifically, the design of insensitive lead fibers and the fabrication of a device to allow both fringe counting and the detection of the change from increasing to decreasing strain or the reverse. This thesis will also investigate the possibility of changing the sensitivity of the sensor by changing its placement in a composite panel.

A literature survey of past and present work with two-mode sensors, both circular-core and elliptical-core, is given in Chapter 2. The fundamental concepts of the two-mode sensor are presented in Chapter 3. Chapter 3 also includes the motivation behind the experimental work. Chapter 4 describes the experimental work performed for this thesis. Specifically, Section 4.1 deals with the insensitive lead fibers, Section 4.2 looks at the

solution to the problems caused by fringing, and Section 4.3 investigates the embedding of sensors between different laminae of a composite panel.

2.0 Literature Survey

This chapter is a literature survey of the work done with two-mode optical fiber sensors. Section 2.1 gives a history of the sensor, including early experiments and theoretical development. A brief summary of the work performed at the Fiber & Electro-Optics Research Center (FEORC) is included in this presentation. Section 2.2 concentrates on the research performed with elliptical-core two-mode fiber sensors.

2.1 A History of the Two-Mode Optical Fiber Sensor

The use of interference between individual modes in a single fiber for sensing purposes was first presented by Layton and Bucaro in 1979 [11]. They used a coil of two-mode fiber as a hydrophone to detect acoustic signals. Theoretically, a general expression for the intensity pattern caused by the interference between any two modes is derived. This expression is then used to calculate the output intensity for the interference of the lower order modes of the fiber. Layton and Bucaro give plots representing the calculated spatial output pattern for interference between the HE_{11} and HE_{12} modes as well as between the HE_{11} and TM_{01} modes. The plot representing the interference between the HE_{11} and TM_{01} modes is nearly identical to the output pattern seen experimentally. Figure 1 is a reprint of the calculated output field for the HE_{11} and TM_{01} modes as given in Layton and Bucaro's paper. The experimental section of the paper deals specifically with the interference between the HE_{11} and TM_{01} modes, the two lowest order modes in a fiber. Some important experimental considerations that need to be underscored are:

- The input conditions have to be properly adjusted in order to excite the proper modes.

- The polarization state of the input light has to be known and linear.

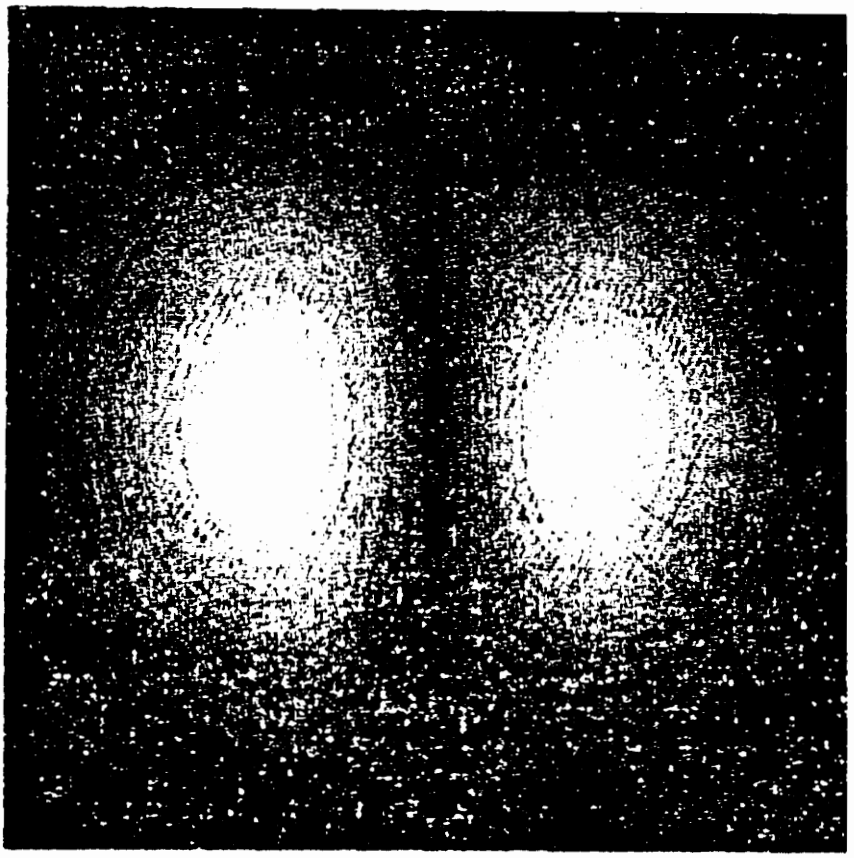

Figure 1. A reprint of the calculated output power pattern of a two-mode fiber as presented by Layton and Bucaro[11].

- A spatial filter placed at the peak intensity point of one lobe of the two-lobe pattern is necessary in order to detect the varying signal.

The authors conclude that the two-mode fiber sensor is less sensitive than a conventional Mach-Zender interferometer, but the two-mode sensor is sensitive enough for most applications. The two-mode sensor also has a lower noise content than the two fiber interferometers. It is pointed out that the fiber used in the experiment has been optimized for communication purposes. The future directions given in this paper include obtaining a fiber where the difference in propagation constants between the two modes was greater, thereby increasing its sensitivity.

In the following years, knowledge of the characteristics of two-mode fibers increased dramatically. Groups studied the propagation characteristics of two-mode fiber and designed methods to determine the modal delay difference between the first two modes of the fiber [12-15]. Known methods for measuring the single-mode cutoff wavelength were re-evaluated and compared [16]. This research helped promote the use of this type of fiber for sensing purposes.

In 1984, a two-mode fiber optic temperature sensor was presented by McMillan and Robertson [17]. The paper details two methods for sensing temperature: fringe-counting and chromatic transmission spectrum analysis. Fringe counting involves counting the number of oscillations, or beats, the interference pattern experiences and determining the

temperature change from this. The focus of their paper is not, however, on intensity modulation caused by the interference of the two-modes in the fiber. The authors surmise that the use of fringe counting is not dependable because of the noise and power fluctuations in the system. Their solution is a sensor based on the analysis of the change in the chromatic transmission spectrum of the fiber. The determination of the chromatic transmission spectrum involves changing the wavelength of the light and measuring the required wavelength change to undergo one complete oscillation in the output intensity. The required change in wavelength is shown to decrease as temperature increases. The main problem with this idea is that a tunable source with a very narrow linewidth is necessary. Although the sensitivity has been shown to increase with the use of the chromatic transmission spectrum method, the increase in cost and complexity of the system makes this method less practical than using the two-mode fiber as an interferometer.

About this time other groups, including the Fiber & Electro-Optics Research Center (FEORC) at Virginia Tech and the Edward L. Ginzton Laboratory at Stanford, started investigating two-mode or few-mode fiber sensors. In the following years, researchers associated with these two groups produced the majority of papers and presentations on few-mode fibers and their applications. A brief summary of the accomplishments of these groups after 1984 in the field of two-mode fiber sensors is presented below.

The work performed at Stanford initially consisted of characterizing the two-mode fiber and designing devices to control and manipulate the modal content of the fiber. The inventions included a two-mode fiber modal coupler[18], a prism output coupling method for few-mode fibers[19], and an evanescent modal filter for two-mode fibers[20]. With these inventions, a complete manipulation of the guided modes in the two-mode fiber was possible. After designing these devices and proving their usefulness, the group at Stanford changed their main focus from circular-core fibers to elliptical-core (e-core) fibers[10]. The reasons for this change will be discussed in Section 3.2. Research in the area of e-core two-mode sensors will be described in Section 2.2.

The work performed at FEORC concentrates mainly on the sensor applications of the two-mode fiber. The specific sensor application developed at FEORC is the sensing of axial strain[7,8,21,22]. When the fiber is attached to a structure, the fiber experiences the same strain as the structure. This strain can then be determined by measuring the changes in the output field of the fiber. Taking this one step further, structural vibrations, which cause strain, can be detected by the two-mode sensor[8].

The method for sensing axial strain is based on the interferometric nature of the two-mode sensor. The two modes in the fiber travel with different propagation constants, causing a varying phase difference between the modes down the length of the fiber. The cross-sectional intensity

distribution within the fiber would indicate the interference between these first two modes and varies down the length of the fiber. The exact nature of this intensity variation will be described in Section 3.1.1. As axial strain is applied to the fiber, the length of the fiber changes. Two other effects produced by axial strain are a change in core size and index of refraction. The combination of these effects essentially causes both modes in the fiber to propagate different distances for different applied strains. As described previously, this change in propagation distance, or pathlength, causes a change in the cross-sectional intensity distribution at the output of the fiber. The precise circular-core theory describing this effect, developed by Safaai-Jazi and Claus at FEORC[23], is presented in Section 3.1.1.

2.2 Recent Work Using E-Core Fibers

The use of e-core fiber for two-mode sensors was first presented by Kim et.al.[10] Using an e-core fiber (core dimensions 2.2 μm $\times$ 4.1 μm), the cutoff wavelengths for the second order even and odd modes are found to be 633 nm and 488 nm, respectively[10]. Therefore, the range of wavelengths allowing only the first order mode and second order even mode to propagate is 488 to 633 nm. Obviously, for fibers with different parameters, i.e. core dimensions and core/clad indices, this wavelength range will differ. The second part of this paper describes the effects of using e-core fiber instead of circular-core fiber for devices such as the modal coupler, the prism output coupler, and the evanescent modal filter. Essentially, these devices are

unchanged by the change from circular-core to e-core fiber.

The major work, presented by Blake et.al., deals with the effect of strain on e-core two-mode fibers[24]. The required deformation necessary for a 2π phase shift between the first and second order modes in a circular-core fiber is first calculated. This formulation is continued by the comparison of the necessary deformation for fibers with different V numbers. The conclusion drawn from this work is that the fiber is more sensitive when the V number is well within the two-mode operating region. Experiments are then performed to determine the necessary deformation required for a 2π phase shift (denoted by $\Delta L_{2\pi}$) when using e-core fiber. The results include graphs showing the comparison between 2π phase shift lengths versus wavelength for different polarizations in the e-core fiber as well as the calculated values for circular-core fiber. These graphs show that the e-core fiber results somewhat follow the circular-core theoretical predictions, but that different polarization states in the e-core fiber give different $\Delta L_{2\pi}$ versus wavelength curves. In all, these results show a need for a rigorous theoretical derivation of the modes in e-core fibers if experimental results are to be compared to theory.

A recent paper deals with the effects of all perturbations, including strain, on e-core two-mode fibers[25]. Briefly, Huang, et. al., calculate the effect of temperature and experimentally try to match the predictions. There is a difference, in the form of a dc offset, between the predicted and experimental results that again demonstrates the need for a theoretical

derivation for the modes in e-core fiber. The theory for a circular-core fiber can only be used to explain the most basic of ideas. The final conclusion of the work is that twisting, squeezing, and bending the fiber has virtually no effect on the phase difference between the modes.

3.0 Fundamental Concepts

Section 3.1 will present the theory for the two-mode sensor. This section will be divided into two parts, one describing the theory for circular-core fiber, and the other describing the theory for e-core fiber. Section 3.2 will explain why e-core fiber was chosen over circular-core fiber for use in two-mode sensors. A typical experimental setup will be described in Section 3.3, and some details about the operation of the sensor will be presented. Section 3.4 will give thorough descriptions of the motivation for the research performed for this thesis.

3.1 Theory of Two-Mode Sensors

3.1.1 Circular-core fiber sensor theory

The theory involves the analysis of linearly polarized (LP) propagation modes[23]. Therefore, a short description of the LP modes is in order. Normally, modes in an optical fiber are either transverse electric (TE), transverse magnetic (TM), or hybrids of these modes (HE or EH). Some of these modes have nearly identical propagation constants, but different cross-sectional field patterns. For the approximation of weakly guiding fibers the core and clad indices are considered nearly equal. This assumption allows a simplification of the mathematical description of the modes in the fiber. The modes with nearly equal propagation constants are in effect combined into single modes. The field distribution of the ℓ^{th} mode in the core of the fiber represented in phasor form is given by

$$\vec{E}_\ell(r,\phi) = A\, J_\ell(Ur/a) \left\{ \begin{matrix} \cos(\ell\phi) \\ \sin(\ell\phi) \end{matrix} \right\} \left\{ \begin{matrix} \hat{a}_x \\ \hat{a}_y \end{matrix} \right\}, \tag{3.1.1}$$

where A is a constant, $U^2 = k_0^2 a^2 (n_1^2 - \beta^2)$, and J_ℓ is the Bessel function of order ℓ. The large parentheses indicate that either the top or the bottom term can be used. This gives a total of four possible solutions for each mode, except for the first mode where the sine term becomes zero and there are only two solutions. These different solutions are equivalent

degeneracies of the mode. As can be seen, each degeneracy has only a x-polarized component or a y-polarized component, and thus the modes are linearly polarized (LP).

Now that the field distribution for each mode is known, we can investigate the interference between the first two modes of the fiber. For a two-mode fiber, the first mode has two degeneracies, and the second mode has four degeneracies. In order to achieve a stable interference pattern at the output, the polarization state of the input light must be linear and contain only one state (either x or y). This reduces the number degeneracies for both modes by a factor of two. Assuming x-polarized input light, the output pattern caused by the interference of the first order mode (LP_{01}) and the even second order mode (LP_{11} even) can now be expressed mathematically. The distributions for these specific degeneracies are given by

$$\vec{E}_{01}(r,\phi) = A_1 \, J_0(U_{01}r/a) \, e^{-j(\beta_{01}z-\Psi_{01})} \hat{a}_x \tag{3.1.2}$$

and

$$\vec{E}_{11}(r,\phi) = A_2 \, J_1(U_{11}r/a)\cos(\phi) \, e^{-j(\beta_{11}z-\Psi_{11})} \hat{a}_x \, , \tag{3.1.3}$$

where $\beta_{\ell m}$ is the propagation constant for the mode and $\Psi_{\ell m}$ is a random phase term. The cross-sectional output intensity distribution of the fiber is then the square of the sum of the two fields and is described by

$$I = I_0 \left[\begin{array}{l} A_1^2 \, J_0^2\left(\frac{U_{01}r}{a}\right) + A_2^2 \, J_1^2\left(\frac{U_{11}r}{a}\right) \cos^2\phi + \\ \quad 2A_1 \, A_2 \, J_0\left(\frac{U_{01}r}{a}\right) J_1\left(\frac{U_{11}r}{a}\right) \cos(\Delta\beta z - \Delta\Psi) \cos\phi \end{array} \right], \tag{3.1.4}$$

where $\Delta\beta$ is the difference between the propagation constants for the two modes and $\Delta\Psi$ is the difference between the random phase terms. Equation (2.4) has three parts. The first part is the intensity of the LP_{01} mode, and the second part is the intensity of the LP_{11} mode. The sum of these two terms gives a constant two-lobe output pattern. The third part is the interference term and can have positive or negative values depending on the value of ϕ. When ϕ is between $-\pi/2$ and $\pi/2$, the term is positive; and when ϕ is between $\pi/2$ and $3\pi/2$, the term is negative. The third term therefore adds to or subtracts from the static field depending on the value of ϕ. As z or $\Delta\beta$ changes, the cross-sectional distribution of this term also varies sinusoidally. The interference term is what creates the varying two-lobe output pattern for the fiber as the fiber is perturbed. Figure 2 shows these the three terms descibed above and the final output pattern for three different values of $\Delta\beta z$.

3.1.2 Theoretical analyses of e-core fibers

The first attempt to derive the modal equations for an elliptical core waveguide was presented in 1962 by C. Yeh[26]. The wave equation is rewritten in elliptical coordinates and solved in terms of Mathieu functions. Furthermore, using the condition that both electric and magnetic field components must be continuous at the core-clad interface, an expression for the field components is derived. Unfortunately this expression consists

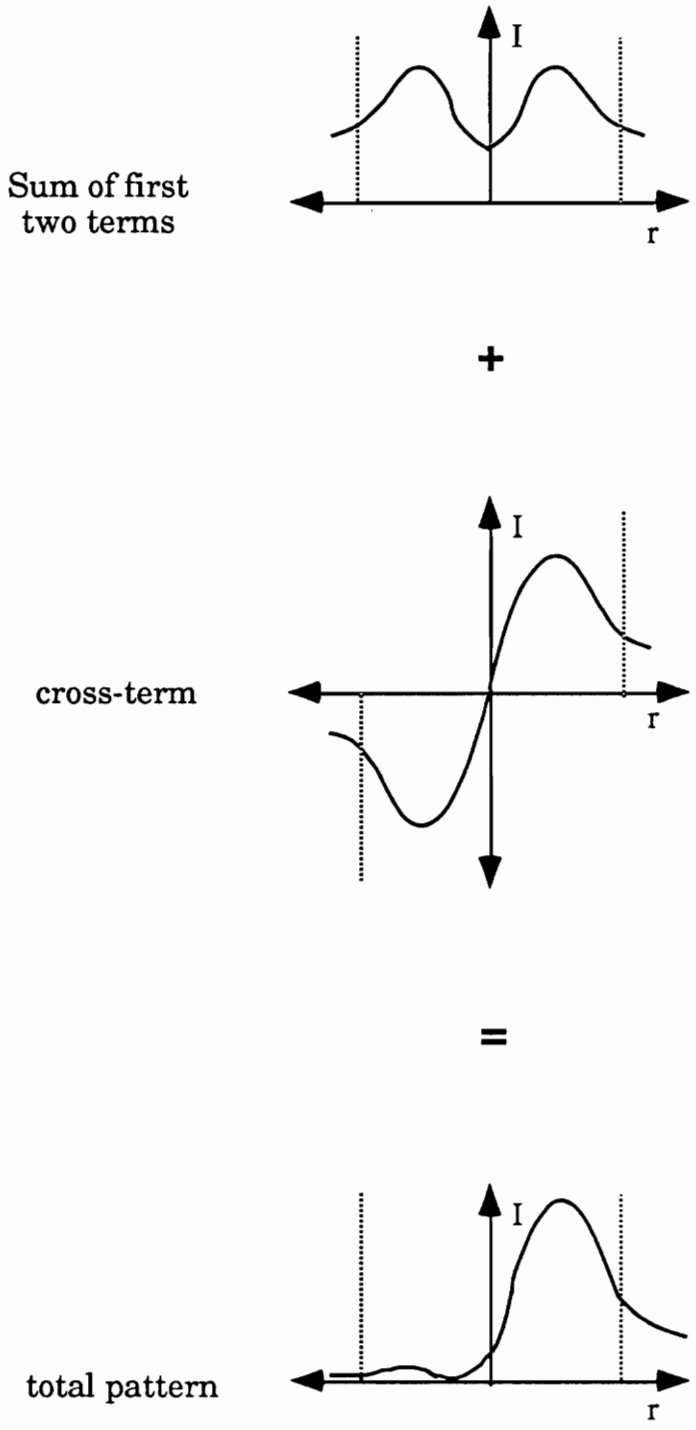

Figure 2(a). Interference pattern construction for $\cos(\Delta\beta z - \Delta\Psi) = 1$.

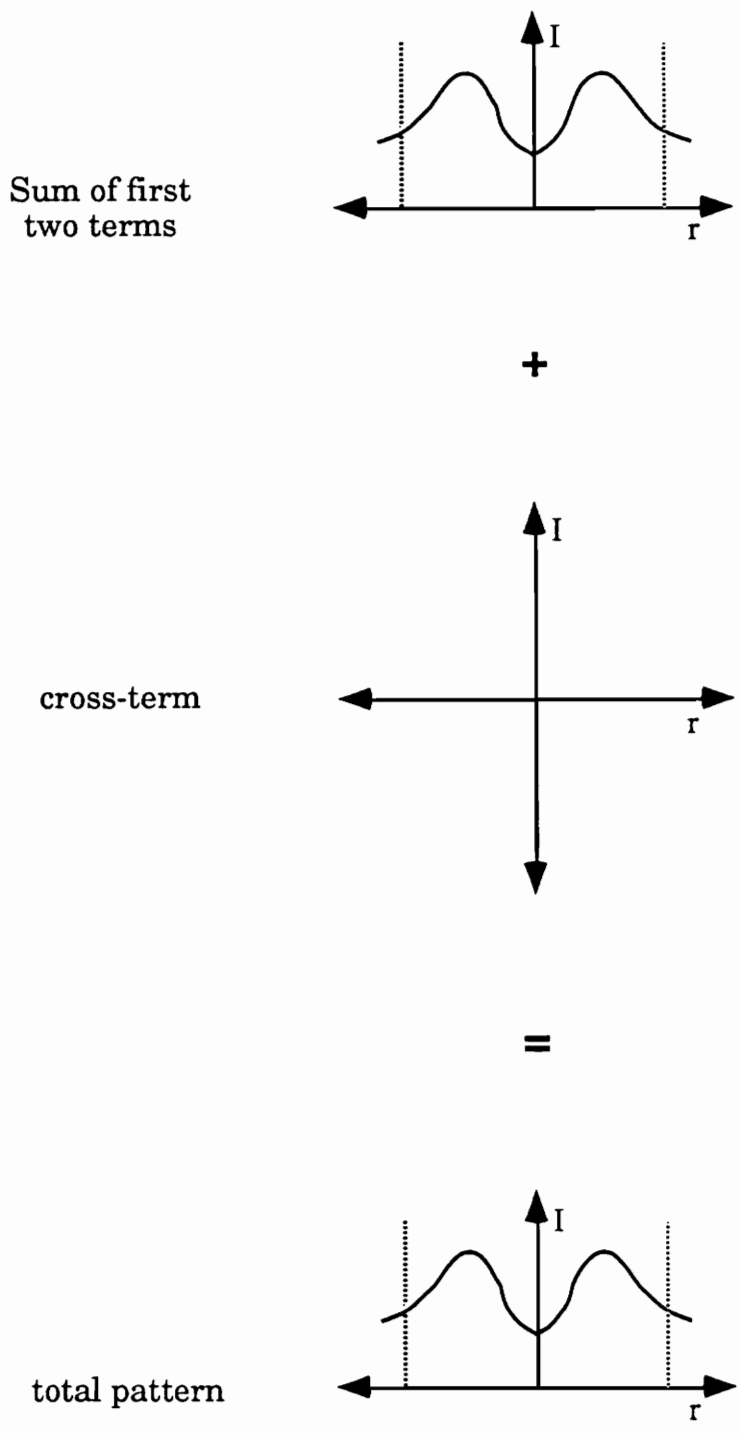

Figure 2(b). Interference pattern construction when $\cos(\Delta\beta z - \Delta\Psi) = 0$.

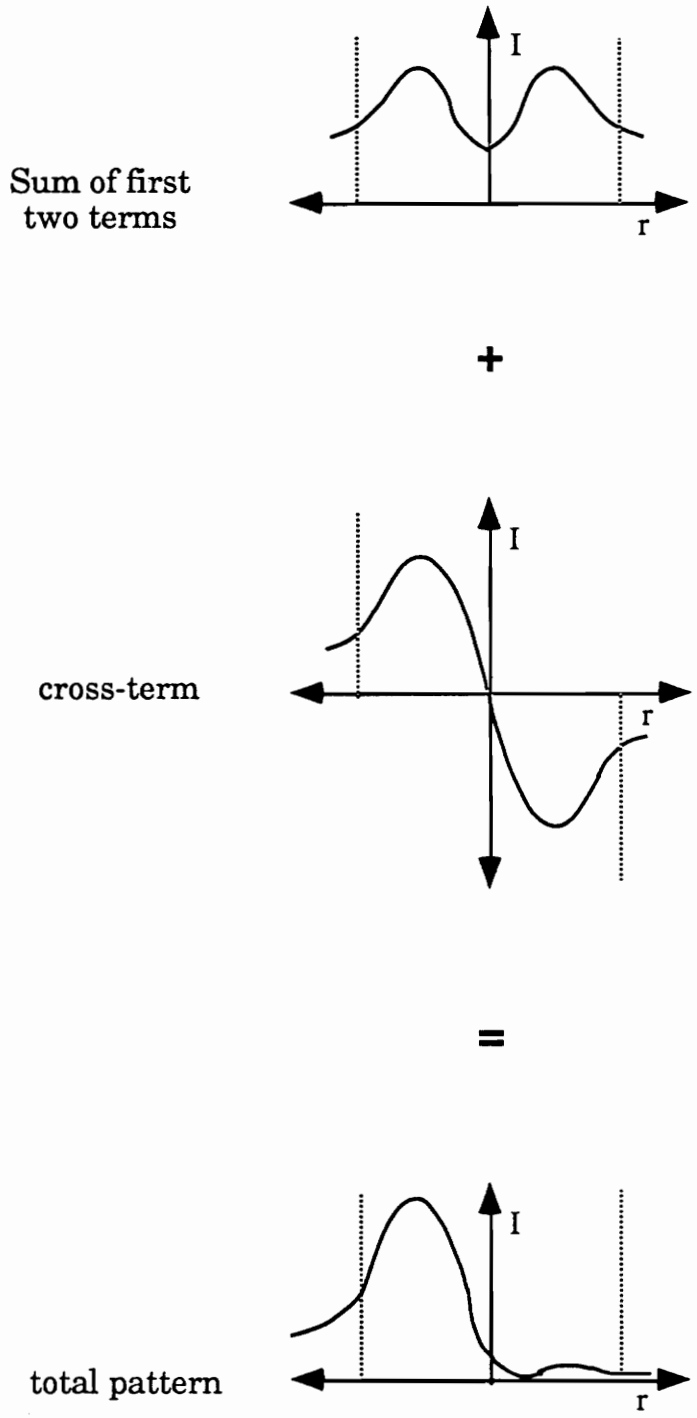

Figure 2(c). Interference pattern construction for $\cos(\Delta\beta z - \Delta\Psi) = -1$.

of Mathieu and modified Mathieu functions, and in order to determine the propagation constant for any mode, an infinite dimensional determinant must be solved. This is done by truncating the determinant numerically to achieve the desired level of accuracy. Although this gives precise results, the amount of work involved to achieve one result is immense.

Another approach for the derivation of the field distributions for modes in a fiber with non-circular core was presented by Gianino, Bendow, and Wintersteiner[27]. This work is an extension of work published earlier by Eyges et al.[28]. The process is to transform the usual Helmholtz differential equations that define the fields into a single integral equation that will approximate any one of the rectangular field components. The field components are then represented as an infinite sum of Bessel functions. This sum can be truncated to six terms with very accurate results. As with Yeh's method, a large amount of numerical computation is needed to define the equation for one mode shape.

In 1986, Snyder and Zheng[29] derived a simple asymptotic solution to Maxwell's equations for fibers of arbitrary cross-section, including e-core fiber. The results of this work include a table representing the modal field distribution for many different core shapes, including elliptical. Cutoff V numbers for fibers with arbitrary core shapes are presented for the first two modes of each fiber. The asymptotic approximation used in this paper is accurate for large V numbers, but gets worse as V decreases. As an example, the authors give a comparison for a circular-core fiber. With a V

number of 2.405 (just at single mode cutoff) the error between the asymptotic solution and the classical solution is just over 2 percent. Although this error is small, some applications do require more accurate results.

The most recent attempt at describing the modal distributions in e-core fiber came from Kumar and Varshney[30]. Their work deals specifically with two-mode e-core fibers. Essentially, the solutions found for a rectangular shaped waveguide are perturbed to arrive at the solutions for e-core fiber. This approximation gives a plot of cutoff V number versus ellipse ratio for the different modes as well as comparisons between effective index and group index differences versus V number for different ellipse ratios. The results are in fair agreement with previous results.

In summary, there have been at least four separate techniques for describing the modal fields in e-core fibers. Three of these methods involve long calculations for each individual mode, and the fourth (Snyder and Zheng) may have too much error due to the approximation used. A good feeling for the modal distribution in an e-core fiber can be obtained, but a simpler method is still needed. Toward this end, researchers at FEORC are presently performing a numerical analysis of e-core fibers that does not involve infinite matrices[31].

3.2 Advantages of E-Core Fibers Over Circular-Core Fibers.

From the outset, researchers using two-mode fiber sensors have noticed the need for very strict input alignment and polarization in order to achieve a clear two-lobe pattern at the output of the fiber[11]. The theory in Section 3.1.1 explains the need for these strict input conditions. The interference pattern seen in the far field of the output is actually the interference between the first order mode and the second order even mode, both modes having the same linear polarization state. When expressed in terms of modes degeneracies, we want only one degeneracy of the "two" LP_{01} modes and one degeneracy of the "four" LP_{11} modes. Although these degeneracies can be excited with careful alignment at the input of the fiber, there is no guarantee that only these degeneracies will be present at the output of the fiber. The uncertainty arises from the internal characteristics of the circular-core two-mode fiber. First, circular-core fiber is not polarization preserving. Therefore small external perturbations may cause the polarization states to vary along the length of the fiber. Although this phenomenon can be used to advantage in polarimetric sensors, it will cause very unstable output patterns in two-mode sensors. Second, the propagation constants for the degeneracies of the second order mode are nearly but not quite equal. Small perturbations to the fiber will therefore cause changes in the cross-sectional intensity distribution of the second order mode. This unstable intensity distribution will lead to instabilities in the far field output pattern of the fiber. Therefore, the same small perturbations that are being measured by the sensor can cause instabilities

in the far field output pattern of the sensor, which will lead to errors in the detected signal.

In order to alleviate these problems, e-core fibers are chosen for two-mode fiber sensors operations[10]. E-core fibers remove both effects that cause instabilities in the output pattern of the fiber. First, an e-core fiber is polarization preserving when the polarization of the input light is parallel to the major axis of the ellipse of the core. This guarantees that the output light will have the same polarization state as the input light. Similarly, the polarization state of the two modes are the same. Second, the propagation constants of the second order even and odd modes are not equal. The LP_{11} odd mode cutoff wavelength is lower than that of the LP_{11} even mode. This gives a range of wavelengths that allow second order even mode propagation but not second order odd mode propagation. Choosing a wavelength in this range and injecting with the correct polarization state gives a very stable cross sectional intensity distribution, and hence a stable two-lobe output pattern.

3.3 A Typical E-Core Two-Mode Experimental Setup

The following is a description of the experimental setup for an e-core two-mode fiber sensor. This is a typical setup for most experiments performed at FEORC. Figure 3 will be used as a reference for the description.

A linearly polarized HeNe laser (λ = 633 nm) is used as the source. A lens

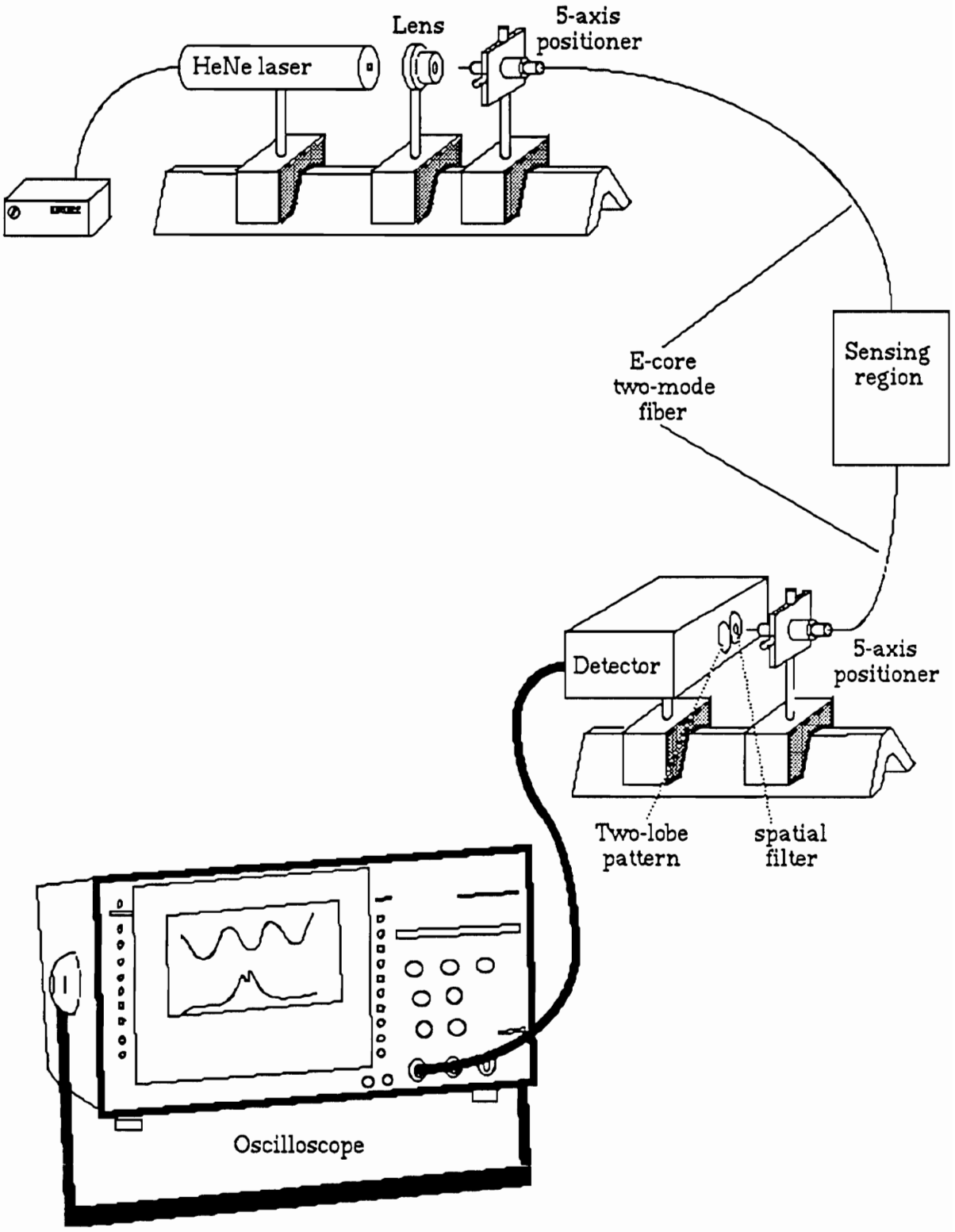

Figure 3. Typical experimental setup for e-core two-mode sensor.

with the same numerical aperture as the fiber is used to focus the light onto the endface of the fiber. To align the endface of the fiber with the focal point of the lens, a five-axis positioner is used. This positioner allows adjustment in the x, y, and z directions as well as in the two rotational directions with axes of rotation parallel to the fiber face, hence five-axes. An important feature of the five-axis positioner is the ability to rotate the chuck, which holds the fiber in position. Although the positioner is not precisely designed for rotation in this manner, it is still easily accomplished. This rotational ability allows alignment of the major axis of the core ellipse and the polarization direction of the source.

The fiber is e-core and two-mode (at 633 nm) manufactured by Andrew Corporation with a single mode cutoff wavelength of approximately 750 nm. This fiber runs from the source to the sensing region and then to the detector. In the sensing region, the fiber may be attached to a vibrating beam, embedded in a graphite-epoxy composite, wrapped around a PZT cylinder, or placed in any other configuration useful for sensing strain or vibration.

At the detector, another five-axis positioner is used for precise alignment of the fiber endface to the detector. Although the five-axis positioner is not required for this alignment, it helps in maximizing signal power and choosing the optimum point for spatial filtering. This spatial filtering occurs because the output pattern has two lobes which oscillate 180° out of phase with one another. Only one of these lobes is needed for sensing

purposes; hence, a spatial filter placed over the face of the detector will limit the output signal to that of one lobe. The detector itself is a simple silicon detector reverse biased and connected to an amplifier. The amplified signal is then fed to an oscilloscope which displays the sensing signal for analysis.

The two-mode sensor can operate in two specific regimes. The sensor is interferometric, which means that it has a sinusoidal periodic output. For large strains, the output will undergo many periods, or fringes. Therefore, the two regimes are the approximately linear regime within one fringe and the non-linear regime. The approximately linear regime occurs when the magnitude of the strain is small enough that only a partial period of the sinusoid is seen at the output. This partial period is centered at the midpoint between maximum and minimum, and the strain is small enough so that the output never crosses a maximum or minimum. The non-linear regime is therefore when the strain causes the output to cross one or more of the maximum or minimum points. This distinction will be discussed further in Section 3.4.2.

3.4 Motivation for Research

3.4.1 Motivation for insensitive lead fibers

The lead fibers, or lead-in and lead-out fibers, are the fibers that run from the source to the sensing region and from the sensing region to the detector, respectively. As shown in Section 3.3, a lead fiber could be the same e-core

two-mode fiber used in the sensing region. In other words, the e-core two-mode fiber runs from the source, through the sensing region, and on to the detector; this presents major problems. First, the lead fibers are sensitive to the same external perturbations as the sensing fiber. Therefore, any vibration in the lead fibers, such as those caused by ambient motor noise, air movements, or temperature changes, can cause changes in the output of the sensor. These changes in the output will most likely be attributed to changes in the sensing region and lead to a misinterpretation of the output of the sensor.

There is another problem that sensitive lead fibers cause in the practical implementation of these sensors. One of the final uses for this type of sensor is in the area of smart structures. This may include the embedding of the sensor in a composite panel in order to sense strain in the panel. If there is a requirement for the sensing of strain in a specific gage length location inside the panel, the sensing region must be isolated. This means that the fiber inside the composite must be sensitive only in the region desired. Obviously, this cannot occur using a single fiber from source to detector. The development of insensitive lead fibers becomes a necessity.

3.4.2 Motivation for in-line beam-splitter

Because the e-core two-mode fiber sensor is an interferometric sensor, its output is periodic in nature. This means that for large variations in strain, the output will go through many fringes or periods. If the sensor is

subjected to vibration, the strain in the fiber will periodically increase and decrease. For large amplitude vibrations, large strains will be present, and the sensor will experience fringing. One of the problems associated with fringing occurs when the sensor output passes through many fringes and the applied strain changes from increasing to decreasing, or vice versa. This "change in direction" may not be picked up by the detection electronics. If the detection electronics count fringes, a change in direction may not be detected. Therefore, the sensor will not be able to sense vibrations accurately.

To remove the possibility of fringing, the sensor is usually operated in its "approximately linear" range. The approximately linear range is the range between the maximum and minimum points of the sinusoidal output pattern. When operated in this region, the output is somewhat linear with strain. In actuality, the output can be chosen to remain increasing with increasing strain and decreasing with decreasing strain. The output is not strictly linear. The "linear" solution does have its problems. First, the sensor rest state must stay at the quadrature point (Q-point), or the midpoint on the sinusoid, which will give the maximum possible range of operation. This range of operation is also limited by the fact that the sensor must stay in the linear range of the sensor. To maintain the sensor in the correct range, the sensing region can be shortened or the vibrational magnitude can be restricted. In all cases, the operation and usefulness of the sensor is restricted.

Figures 4, 5, and 6 demonstrate the process of fringing. Figure 4 shows the operation of the sensor in the approximately linear range. The signal corresponding to strain due to vibration is the bottom curve, and it is translated through the sinusoid representing output power versus strain. This gives the signal of output power versus time on the right. If the amplitude of vibration is increased, as in Figure 5, the output signal variation is greater than one half period and "dips" at the top and bottom of the signal are present. As the amplitude of vibration is increased, the "dips" get larger (Figure 6) and fringing is very evident. As can be imagined, the presence of these nonlinearities with large vibrational amplitudes will cause problems if the sensor is to be operated in the linear range. Similarly, if the sensor employs fringe counting techniques, there is a good possibility that the change from increasing strain to decreasing strain may be missed at the point of inflection.

To overcome these problems, an optical scheme to allow fringe counting without ambiguity is presented. An in-line beam splitter is designed to give two output signals 90° out of phase with one another. An important quality of this design is that when strain is increasing, one signal will always come to the minimum and maximum points on the sinusoid after the other (lagging), and when the strain is decreasing, the signal that was lagging will always come to these minimum and maximum points before the other (leading). Figure 7 uses the translation described above to show the lead-lag quality of this design. There are two power versus strain curves for the sensor to denote the two out-of-phase signals. With the proper detection

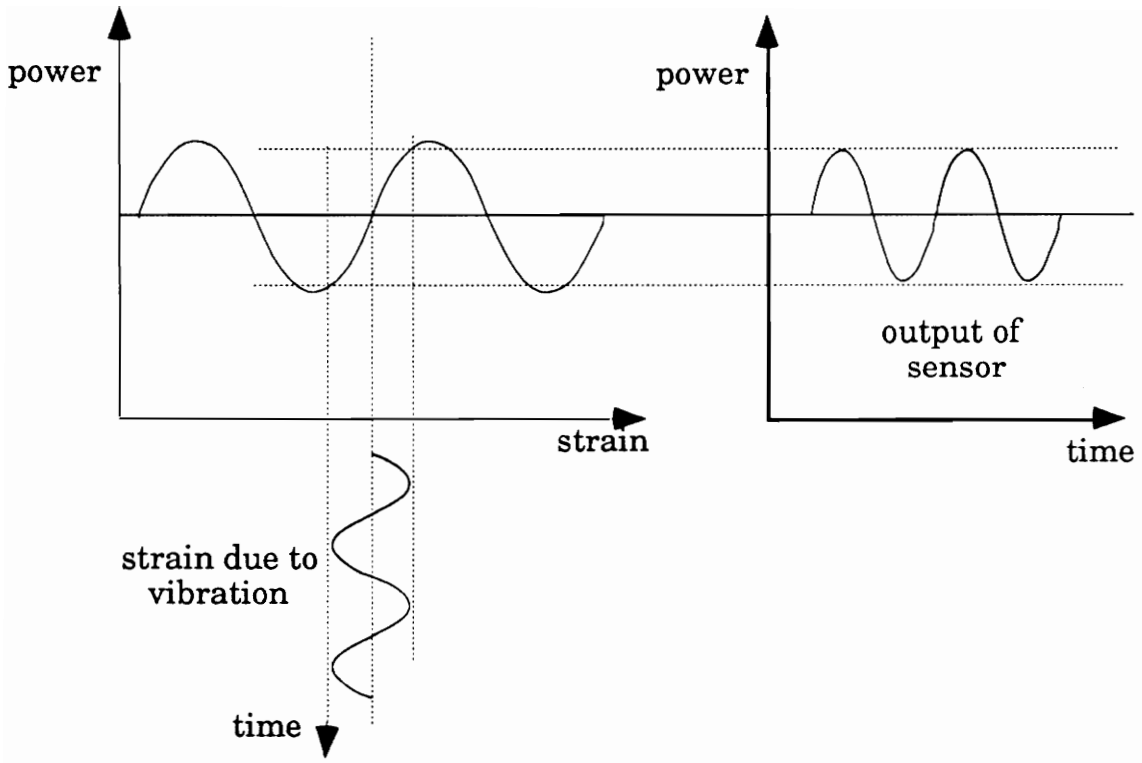

Figure 4. Translation of strain due to vibration through the strain vs. power curve of the sensor. The result is the output power vs. time curve of the sensor due to the vibration.

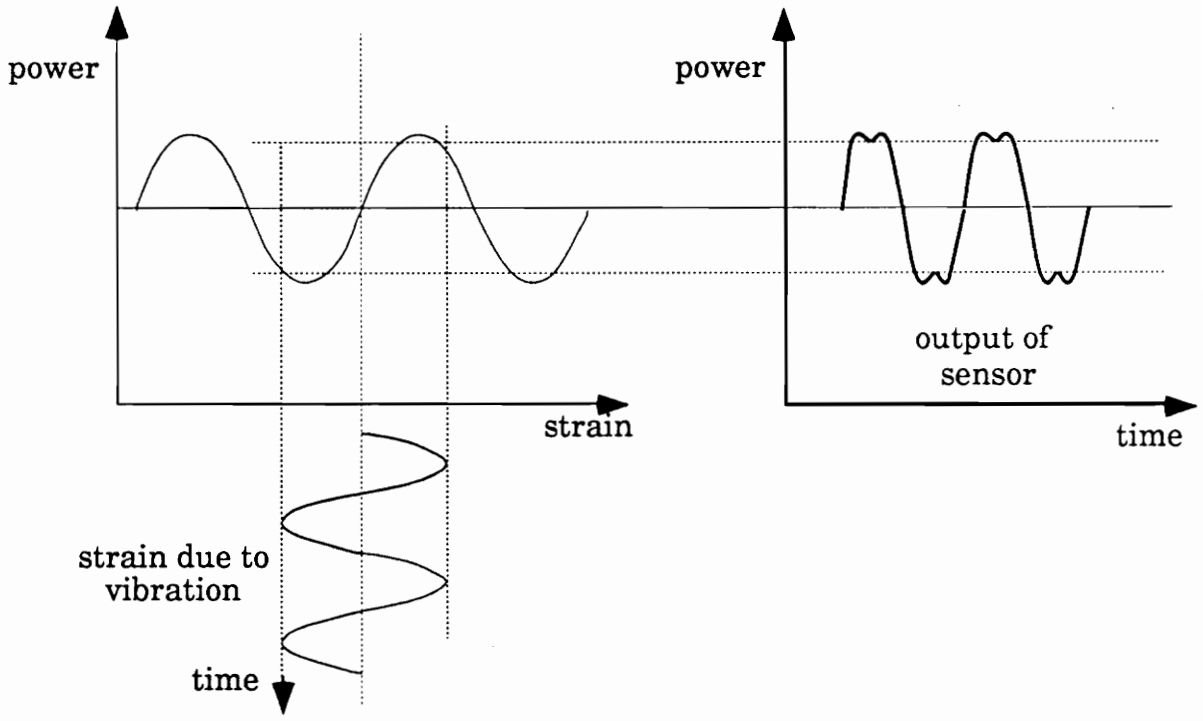

Figure 5. Translation of larger amplitude vibration through strain vs. power graph of the sensor. The onset of fringing is noticeable.

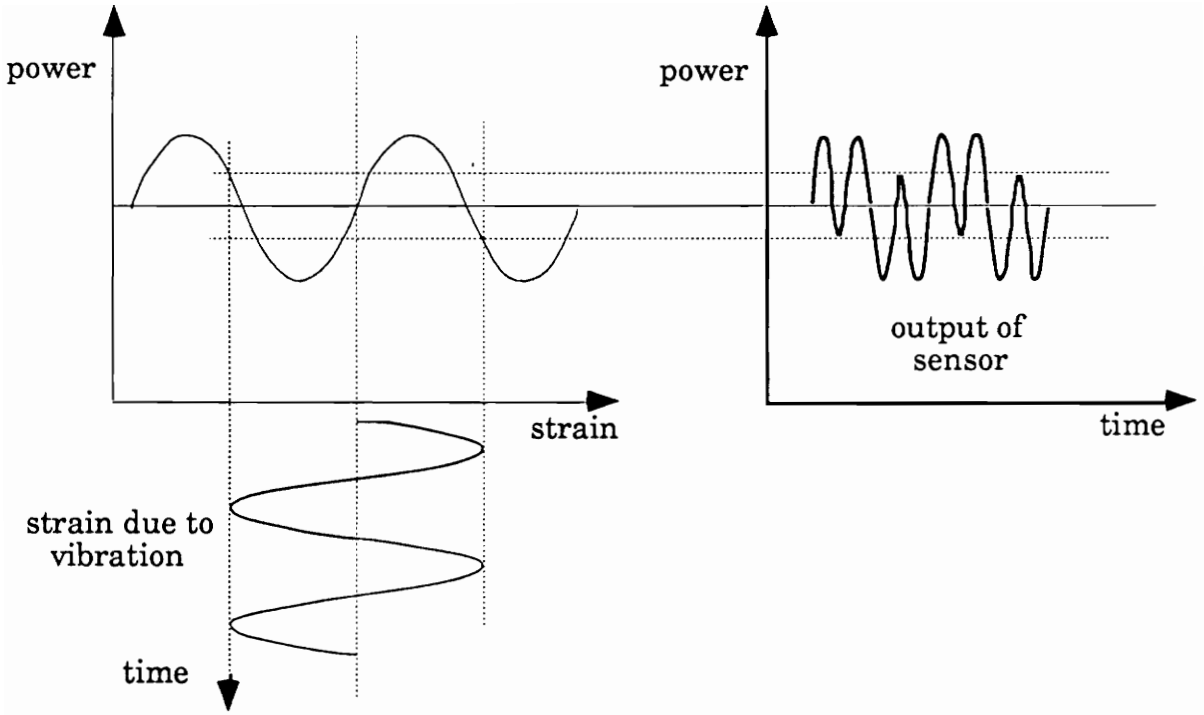

Figure 6. Translation of still larger amplitude vibration through the strain vs. power curve of the sensor. At this point, fringing is very evident.

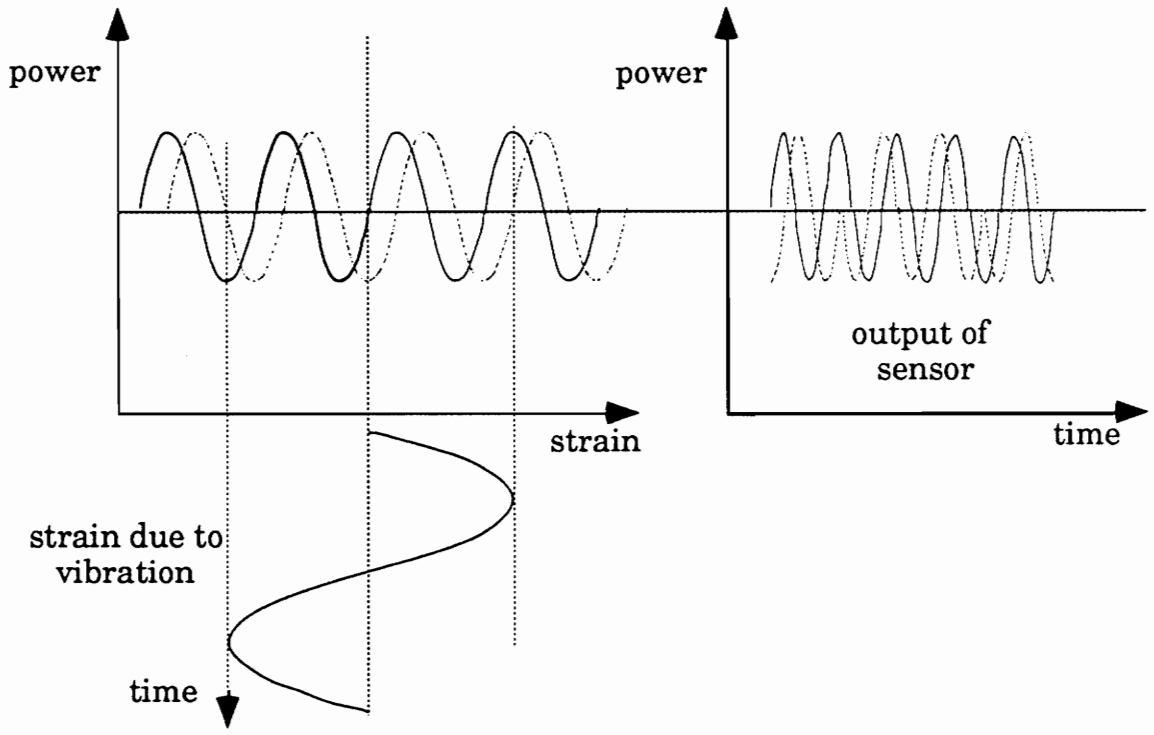

Figure 7. Translation of very large amplitude vibration through strain vs. power curves of two sensors 90° out of phase. Notice the dashed curve starts off lagging the solid curve, changes to leading when the strain changes from increasing to decreasing, and returns to lagging when strain returns to increasing.

electronics, the sign of the strain (increasing or decreasing) can be determined, and vibration sensing can be accomplished for any amplitude of vibration. In fact, by using longer sensing lengths and passing the fiber through the sensing region many times, the sensitivity of the sensor can be increased.

3.4.3 Motivation for embedded sensor research

Smart structures research includes the ability to perform nondestructive evaluation of the structure. The major focus of this effort has been to embed fiber optic sensors in composite panels for health monitoring. An improvement in the understanding of embedded e-core two-mode fiber sensors is useful in the development of such concepts.

Prior to the possibility of fringe counting the modal domain sensor fiber response was maintained in the approximately linear range to allow the determination of direction, increase or decrease, of strain in the fiber. This also allowed a simpler method for vibration control implementation using this sensor. In order to keep the sensor in the linear range, its sensitivity to the external perturbation being measured must be strictly controlled. A simple method for changing the strain sensitivity of the sensor is to move it further from or nearer to the neutral axis of the structure. Obviously, the further from the neutral axis the fiber is, the larger the strain it will experience. The following work was done to test the ability to determine the amount of increase or decrease in sensitivity when a sensor is placed at

different positions in a composite panel.

With the development of the beam-splitter presented in Section 4.2, the necessity of being in the linear range for the sensor is no longer present. However, the knowledge of the change in sensitivity based on location in the composite will still be valuable. If the resolution of the sensor is not high enough for the specific application, understanding the amount of change in sensitivity based on placement will allow the proper relocation of the sensor in order to increase the resolution of the sensor to the desired value.

4.0 Experiments

The devices and research designed to make the e-core two-mode sensor more practical are discussed in this chapter. Section 4.1 describes the research performed with insensitive lead fibers. Section 4.1.1 presents the design and Section 4.1.2 presents the fabrication of the insensitive leads. Sections 4.1.3 and 4.1.4 describe experiments performed to test the insensitivity and practicality of the lead fibers. Section 4.2 discusses the in-line beam-splitter which is designed to allow fringe counting as a technique for vibration detection. Sections 4.2.1 and 4.2.2 describe the design and fabrication of the in-line beam-splitter, respectively. Section 4.2.3 details an experiment designed to demonstrate the capabilities of the beam-splitter. Section 4.3 describes the research performed to advance the knowledge about the effect of fiber placement in a composite on the sensor. Section 4.3.1 presents the experiment performed to test the sensitivity of the sensor when placed between different laminae of the composite panel. Section 4.3.2 is a qualitative discussion of the results of the experiment and possible reasons for error in the results.

4.1 Insensitive Lead Fibers

4.1.1 Design

The fiber chosen for the lead-in fiber is an e-core fiber that is single-mode at 633 nm, the operating wavelength of the sensor. An e-core fiber is chosen in order to meet the polarization requirements of the sensing fiber. As stated in Section 3.1.1, the polarization state of the input light to the sensing fiber must be linearly polarized in order to excite only one polarization degeneracy for each mode. The e-core fiber is polarization preserving when injected with light linearly polarized parallel to the major axis of the core ellipse, which is why it is chosen as the sensing fiber. Therefore, using another e-core fiber for the lead-in maintains the polarization state of the source at the input of the sensing fiber. A single-mode fiber was chosen to meet the insensitivity requirements for the lead-in fiber. The output of a properly injected single-mode e-core fiber does not change in intensity or polarization state when placed under external strain. This allows a constant intensity and polarization state at the input of the sensing fiber.

The lead-out fiber is also single-mode at 633 nm, but it is a circular-core fiber. Again, the fiber is single mode because the intensity at the output will not change with external strain. However, the lead-out fiber is not required to be polarization preserving. The output of the sensing fiber is an intensity modulated signal, and the intensity is the only parameter required for processing. There is a requirement on the placement of the core of the

output fiber with respect to the core of the sensing fiber. Since the output of the sensing fiber consists of two lobes oscillating 180° out of phase with one another, the total intensity of the signal does not vary. Observing one lobe gives the required information. Therefore the core of the lead-out fiber must be offset with respect to the core of the sensing fiber in order to pick up only one lobe of the two-lobe pattern.

The attachment of the lead fibers to the sensing fiber must also meet certain requirements. The main requirement is that the bond between the lead fibers and the sensing fiber must be strong. Since the point where the lead fibers and sensing fiber are attached may undergo strain, it must survive the same strains as the fiber. More obviously, the spatial relationship of the cores of the lead fibers and the sensing fiber can not change. If this were to change, the output of the sensor would change and erroneous readings would occur. For these reasons, a fusion splice is chosen as the means to attach the lead fibers and the sensing fiber. The fusion splice is permanent and provides a connection region which is stronger than that produced by any other splicing method since the two fibers are actually fused together.

4.1.2 Fabrication

The following is a step-by-step description of the fabrication of a lead-insensitive, e-core two-mode sensor. The procedure outlined is designed for optimum sensor operation upon completion. The lead-out fiber is first spliced to the sensing fiber. Then the lead-in fiber is spliced to the sensing

fiber.

Step 1: Splicing the lead-out and sensing fibers.

- Wrap the sensing fiber tightly around a PZT cylinder and apply an ac voltage to the electrodes of the cylinder to create a varying strain in the sensing fiber.
- Align the sensing fiber to the laser.
- Using an analyzer, check the polarization state of the output. Rotate the chuck in the 5-axis positioner until maximum linearity of polarization is achieved at the output. (This ensures correct operation of the sensing fiber.)
- Place the output end of the sensing fiber in the fusion splicer.
- Position one end of the lead-out fiber in front of a detector which is connected to an oscilloscope.
- Place the other end of the lead-out fiber at the other side of the fusion splicer.
- Using the micropositioners on the fusion splicer, align the sensing fiber output end and the lead-out fiber input end to achieve the maximum modulation depth on the oscilloscope. (This ensures that the lead-out fiber is picking up one lobe of the two-lobe pattern.)
- Fuse the fiber ends together.
- Remove the two fibers from the splicer.

Step 2: Splicing the lead-in and sensing fibers

- Align one end of the lead-in fiber to the laser.
- Using the analyzer as before, rotate the chuck until the output light has maximum linearity of polarization.
- Place the output end of the lead-in fiber on the fusion splicer.
- Place the input end of the sensing fiber on the other side of the splicer.
- Position the output of the lead-out fiber in front of a power meter.
- Turn off the function generator connected to the PZT for the next step.
- Using the micropositioners on the splicer, align the lead-in and sensing fibers to achieve maximum power output.
- Re-position the output of the lead-out fiber in front of the detector.
- Turn on the function generator in order to see the modulation depth.
- Rotate the lead-in fiber with respect to the sensing fiber. After each small rotation, readjust micropositioners to achieve maximum modulation depth. Continue the rotational process until the absolute maximum modulation depth is achieved. (This ensures that the major axes of the lead-in and sensing fibers are aligned.)
- Fuse the fiber ends together. The sensor is complete.

4.1.3 Experiment and results

This section will describe an experiment designed to test the insensitivity of the lead fibers. The specific fiber used for this experiment will be described first. The e-core sensing fiber is made by Andrew Corporation and has core dimensions 1.25 x 2.5 microns. There is a depressed cladding approximately four times the dimensions of the core. The fiber is single-mode at 850 nm and two-mode at 633 nm with a single mode cutoff wavelength around 700 nm. The outer cladding diameter is 80 microns. The lead-in e-core fiber is nearly identical to the sensing fiber except it is single-mode at 633 nm. The lead-out fiber is a single mode fiber at 633 nm with a core diameter of 4 microns and a cladding diameter of 125 microns.

The first part of this experiment deals with the characterization of the sensing fiber. Specifically, the change in length necessary for a 2π phase shift, $\Delta L_{2\pi}$, is determined. As shown in Figure 8, the fiber is wrapped around two cylinders separated by a certain distance. One cylinder is attached to a micropositioner. These cylinders prevent the fiber from slipping while under stress. The fiber ends are aligned to the laser and to a power meter with a spatial filter. The spatial filter allows the detection of only one lobe of the output pattern. The micropositioner is then moved 12.5 μm at a time, which is the smallest step on the micrometer, and the power level is recorded at each step. The values of power at each step are plotted and $\Delta L_{2\pi}$ is determined from the graph. This test was performed many times with different lengths of fiber and the average for $\Delta L_{2\pi}$ was

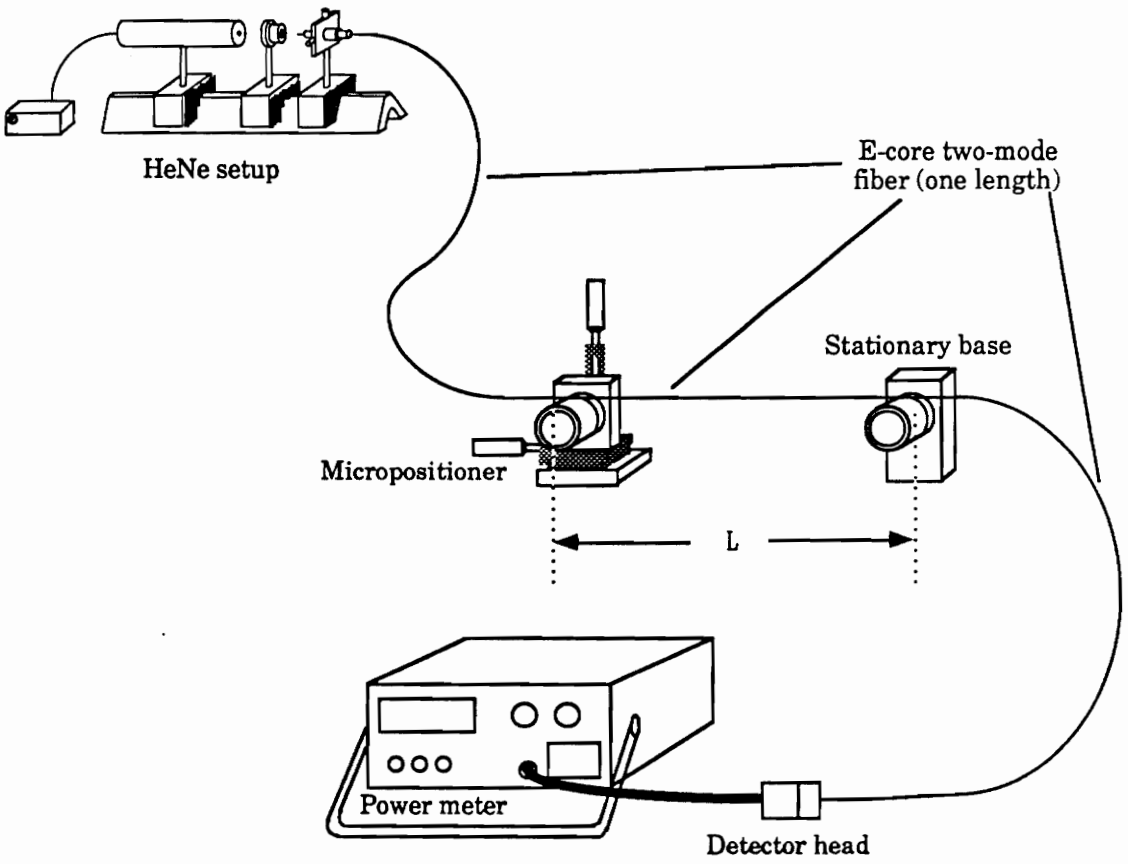

Figure 8. Experimental setup to find $\Delta L_{2\pi}$ for test fiber.

determined to be 101.6 microns. This value will be used for the remainder of the experiment to determine the insensitivity of the leads for an insensitive lead sensor.

In the next part of the experiment, four insensitive lead sensors were fabricated, each having a different sensing fiber length. These sensors were wrapped around two cylinders as before. In this case, the fiber between the cylinders consisted of a small length of lead-in fiber, the sensing fiber, and a small length of lead-out fiber as shown in Figure 9. The splices in the sensors were strain relieved by using capillary tubes and epoxy. This ensured that there was no possibility of changes in the splice causing changes at the output. The lengths for each section of fiber in each sensor are shown in Table 1. The micrometer was again moved 12.5 μm at a time and a power reading was taken at each step. There were only two lasers for use in this experiment, so the experiment was performed four times, each sensor therefore being tested twice. The two data sets for each sensor were averaged and the averages plotted. These plots then gave the $\Delta L_{2\pi}$ for each sensor.

The results of these experiments are plotted on separate graphs and can be seen in Figures 10 through 13. Figures 11 and 12 are nearly identical due to the nearly equal sensing lengths for sensors two and three. These results are then compared to the result of the first part of the experiment in the following way. The deformation in each sensor can be described by

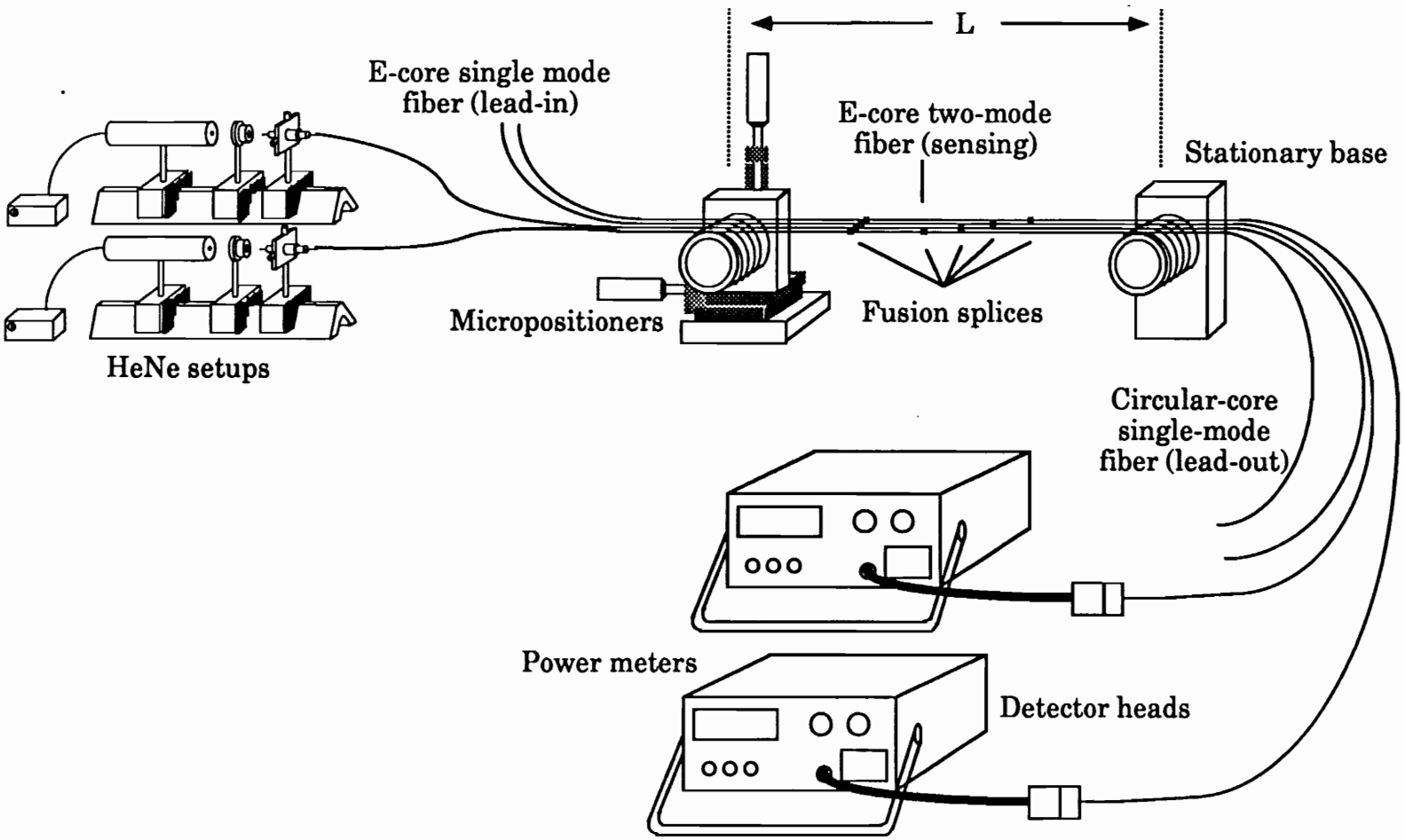

Figure 9. Experimental setup for the testing of four insensitive lead sensors.
Each sensor has a different sensing length.
Note that only two sensors can be tested at one time.

Table 1. Table of lengths of each section of fiber for each sensor.

Sensor #	L_1(cm)	L_2(cm)	L_3(cm)	L(cm)
1	23.5	11.0	50.0	84.5
2	24.0	21.5	38.0	83.5
3	24.0	24.0	36.0	84.0
4	24.2	41.0	18.0	83.2

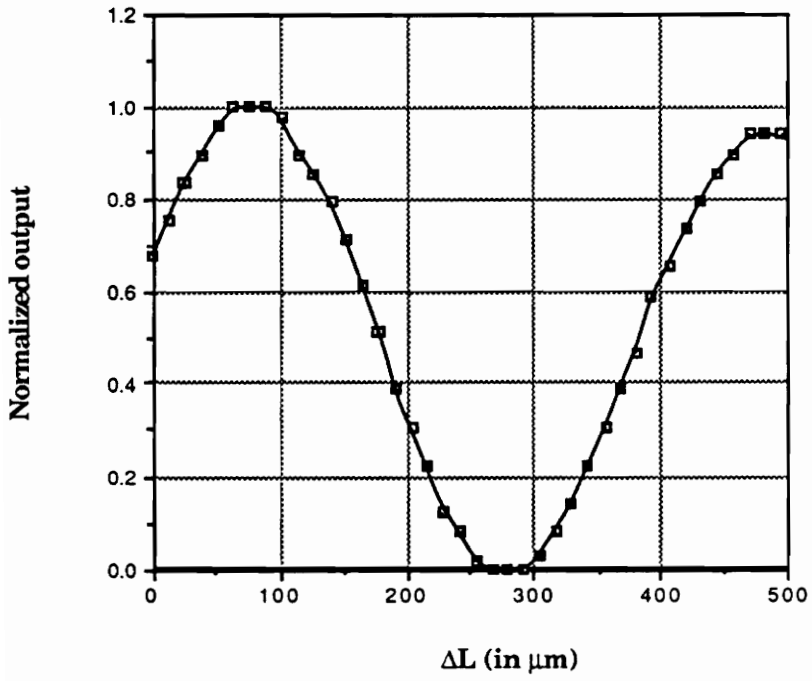

Figure 10. Normalized graph of output power vs. ΔL for sensor 1 (sensing length = 11 cm).

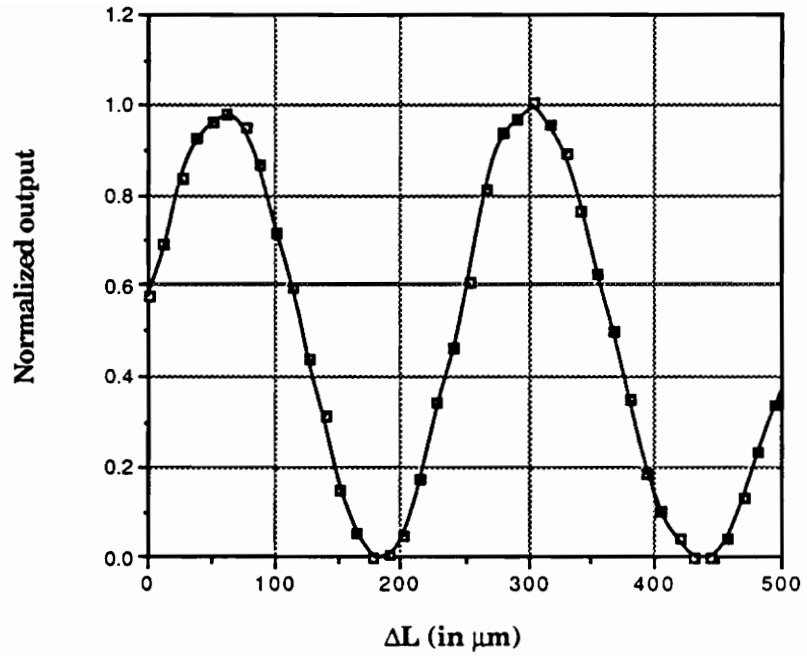

Figure 11. Normalized graph of output power vs. ΔL for sensor 2 (sensing length = 21.5 cm).

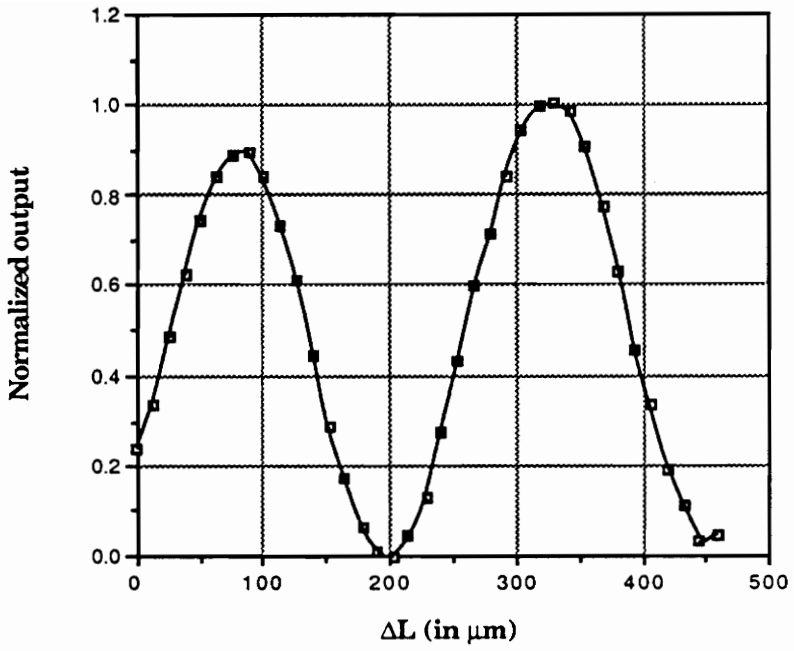

Figure 12. Normalized graph of output power vs. ΔL for sensor 3 (sensing length = 24.0 cm).

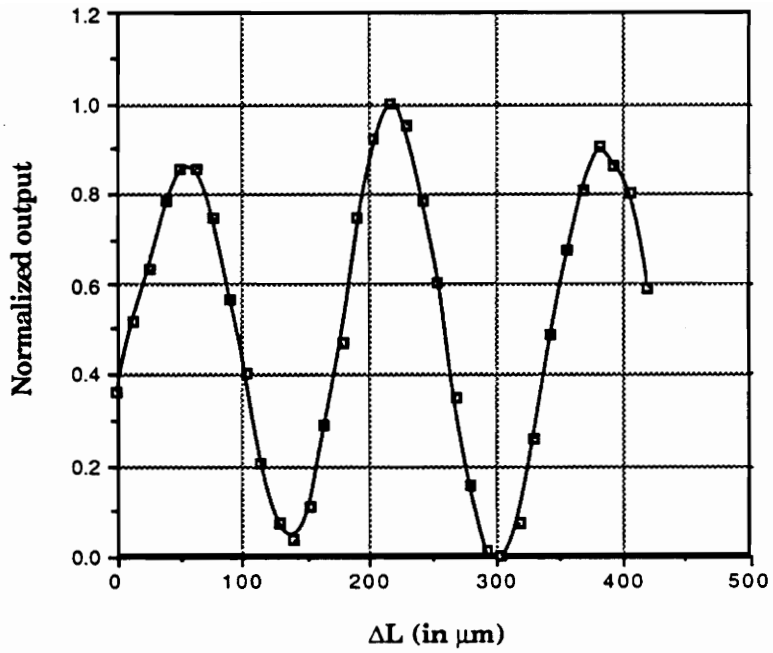

Figure 13. Normalized graph of output power vs. ΔL for sensor 4 (sensing length = 41.0 cm).

$$\Delta L = \sum \frac{P_i L_i}{A_i E_i} , \tag{4.1.1}$$

where P = force applied to the ends of the fiber, A = cross-sectional area of the fiber, L = length of the fiber, E = Young's modulus of the fiber, and the subscript *i* denotes the section of fiber. Assuming that Young's modulus is the same for all three sections of fiber and knowing that the force is the same, the percentage of the total deformation in each section can be determined. Since the sensing fiber is the fiber of interest, the percent deformation in section 2 (sensing fiber) is given by

$$\%\Delta L_2 = \frac{\frac{L_2}{A_2}}{\sum_{i=1}^{3} \frac{L_i}{A_i}} \times 100 . \tag{4.1.2}$$

Using the 101.6 micron value for $\Delta L_{2\pi}$ found in part one of the experiment, the total deformation for each sensor required for a 2π phase shift can be determined. The deformation for each sensor is given by

$$\Delta L_{2\pi} = \frac{101.6\mu}{\%\Delta L_2 \times 0.01} . \tag{4.1.3}$$

Table 2 gives the calculated values for $\%\Delta L_2$, calculated $\Delta L_{2\pi}$, measured $\Delta L_{2\pi}$, and the error for each of the four sensors.

The final part of the experiment tested the effect of straining the lead fibers on the sensor performance. One of the four sensors described above was chosen and the lead in fiber was positioned between the two cylinders (same setup as Figure 8 or 9). The micrometer was moved 12.5 μm at a time, as before, and the power readings were taken. This test was performed again

Table 2. Table of experimental and calculated values for $\Delta L_{2\pi}$ along with % error.

Sensor	1	2	3	4
%ΔL in section 2	25.9	41.7	44.6	60.2
Calculated $\Delta L_{2\pi}$ (in μm)	392.6	243.7	227.6	168.7
Experimental $\Delta L_{2\pi}$ (in μm)	393.7	266.7	241.3	165.1
Error (in %)	0.3	8.6	5.7	2.2

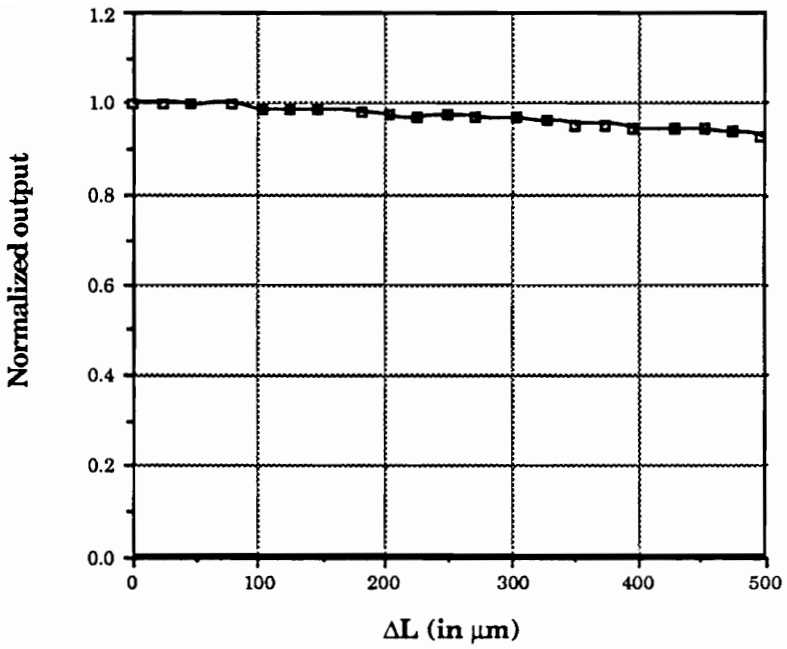

Figure 14. Normalized graph of power vs. ΔL for lead-in fiber only.

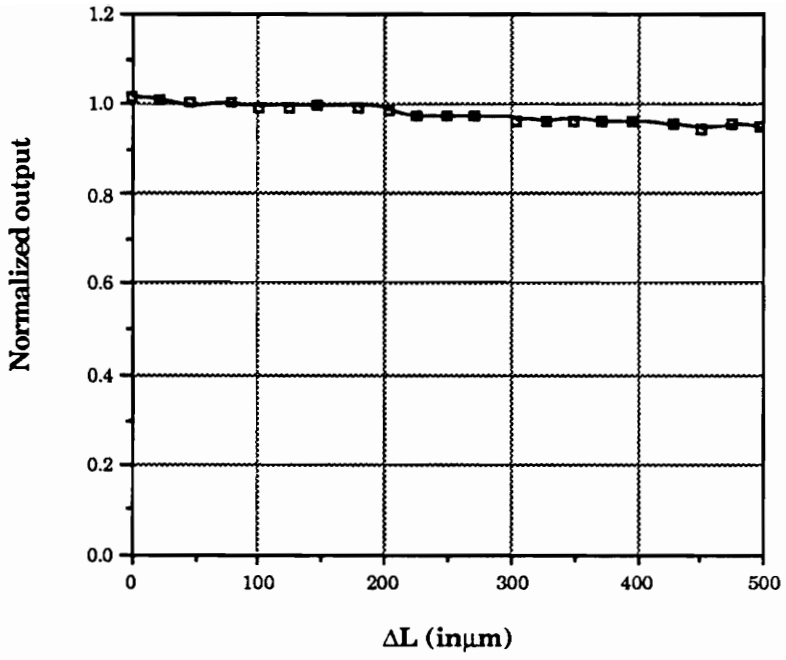

Figure 15. Normalized graph of output power vs. ΔL for lead-out fiber only.

with the lead-out fiber between the two cylinders. Plots of the results of this experiment are shown in Figures 14 and 15. The overall drop in power may be caused by the curve of the fiber around the cylinders.

4.1.4 Embedding of insensitive lead sensors

As stated before, the final use of the e-core two-mode fiber sensor may be as an embedded sensor for use in smart structures. It is therefore useful to determine the effect of embedding an insensitive lead fiber in a composite panel. A graphite-epoxy composite was used, and a conventional e-core two-mode sensor was embedded next to the insensitive lead sensor for comparison. The result of most importance for this experiment was that the fusion splices, which were not protected, survived the embedding process. This means that the insensitive lead fiber is a viable option for embedded sensors.

The second part of the test was to use both sensors and compare them when the composite panel was placed under vibration. The setup for this is shown in Figure 16. A number of vibrational tests were performed with nearly identical results. A sample oscilloscope trace for both sensors is shown in Figure 17. This trace shows that the insensitive lead sensor operates as well or better than the conventional sensor, both in the time and frequency domains. If the trace in Figure 17 is inspected closely, it can be seen that the conventional sensor has some drift in the dc level of the signal. The insensitive lead sensor does not have this drift.

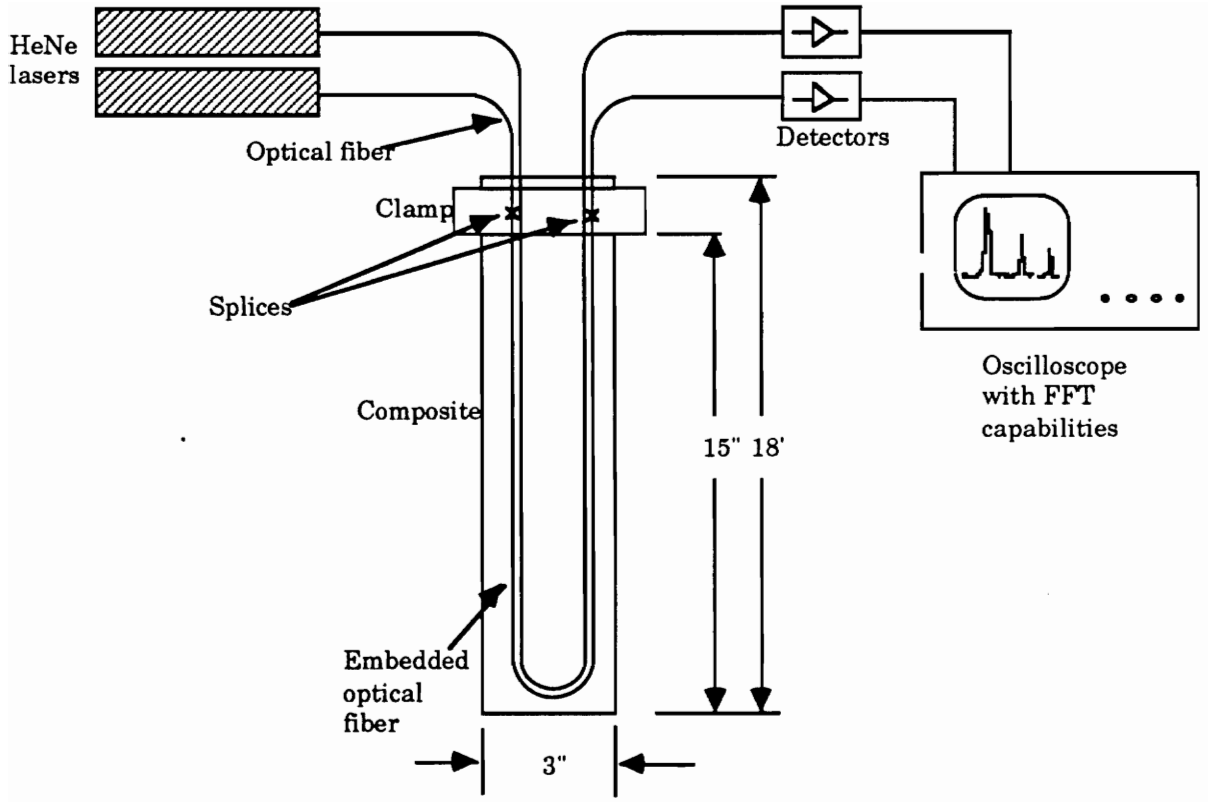

Figure 16. Experimental setup for the testing of embedded insensitive lead e-core two-mode sensor.

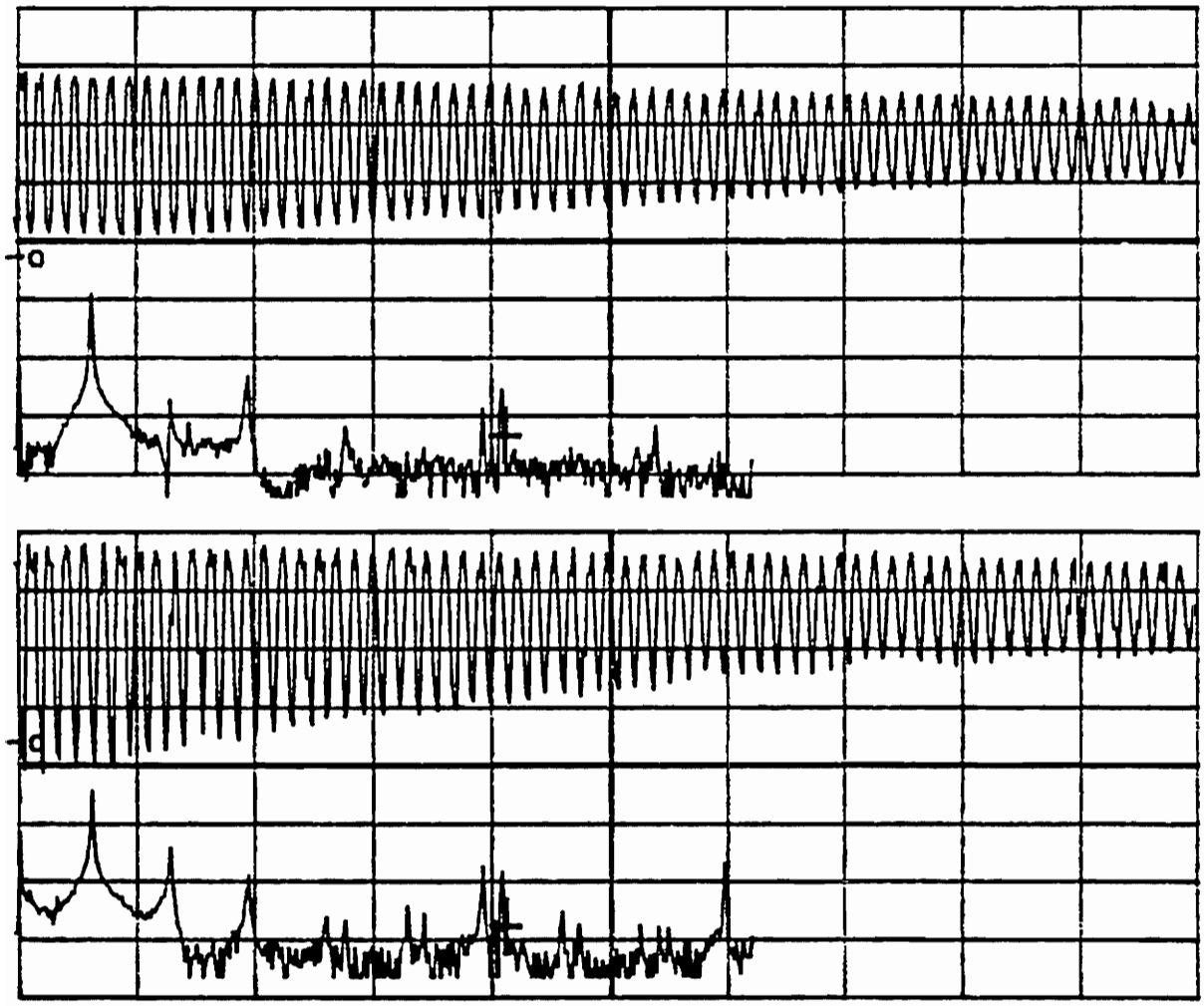

Figure 17. Oscilloscope trace of the outputs from the two sensors. The top trace is the insensitive lead sensor, the bottom is the conventional sensor. The Fast Fourier Transforms of both signals are shown underneath each signal's trace.

4.2 The In-Line Beam-Splitter

4.2.1 Design

In order to achieve two signals which are 90° out of phase with one another, some form of tap-off must be designed for the e-core two-mode fiber. The tap-off is necessary because one signal must continue in the e-core fiber so that its phase will change. The specific design chosen here will employ Fresnel reflections at an angled interface to achieve the two signals. In this respect, it resembles a beam-splitter. The fiber will be cleaved into two pieces, each of which will be polished at 45°. When placed together again, the small air gap that is present will create a reflection perpendicular to the fiber. A second part of the signal will propagate into the second length of fiber. By straining the second length of fiber or changing its length, the phase of its output pattern can be changed to the desired quantity. This gives two signals, one reflected and one transmitted, whose phases with respect to one another can be chosen.

After the sensing fiber has been cleaved, a method for creating the 45° end faces must be designed. Each fiber is placed between two small, glass slides and epoxied in place. Glass is chosen because the reflected signal must propagate through the slide and then be detected. These slides are then polished at the proper angle. Because the fiber is epoxied between the slides, it will also be polished at the angle chosen for the slides. These two pieces can now be realigned to achieve maximum coupling between the

fibers. It is also possible that an index matching fluid may be necessary between the fiber endfaces to help balance the percentage of light reflected with the amount transmitted. A 50/50 split is the optimum.

4.2.2 Fabrication

The method developed for the fabrication of an in-line beam-splitter will be discussed in this section. The only piece of equipment that had to be designed especially for this method was a holder used to polish specimens at an angle. Because a 45° angle is used for the beam splitting, a holder designed for polishing at 45° was necessary. Figure 18 is a schematic of the polishing jig designed for polishing at an angle. The specimen holder rotates so that any angle, within the range of movement, can be chosen for polishing.

The first step in the process is to make the four small glass slides used to hold the fiber in place for polishing. For the beam-splitters made for the experiments of section 6.4, large microscope slides were cut down to the desired size. An angle was polished on one end of each of these slides so that when aligned later, the beginning of the stripped fiber region can be protected by epoxy.

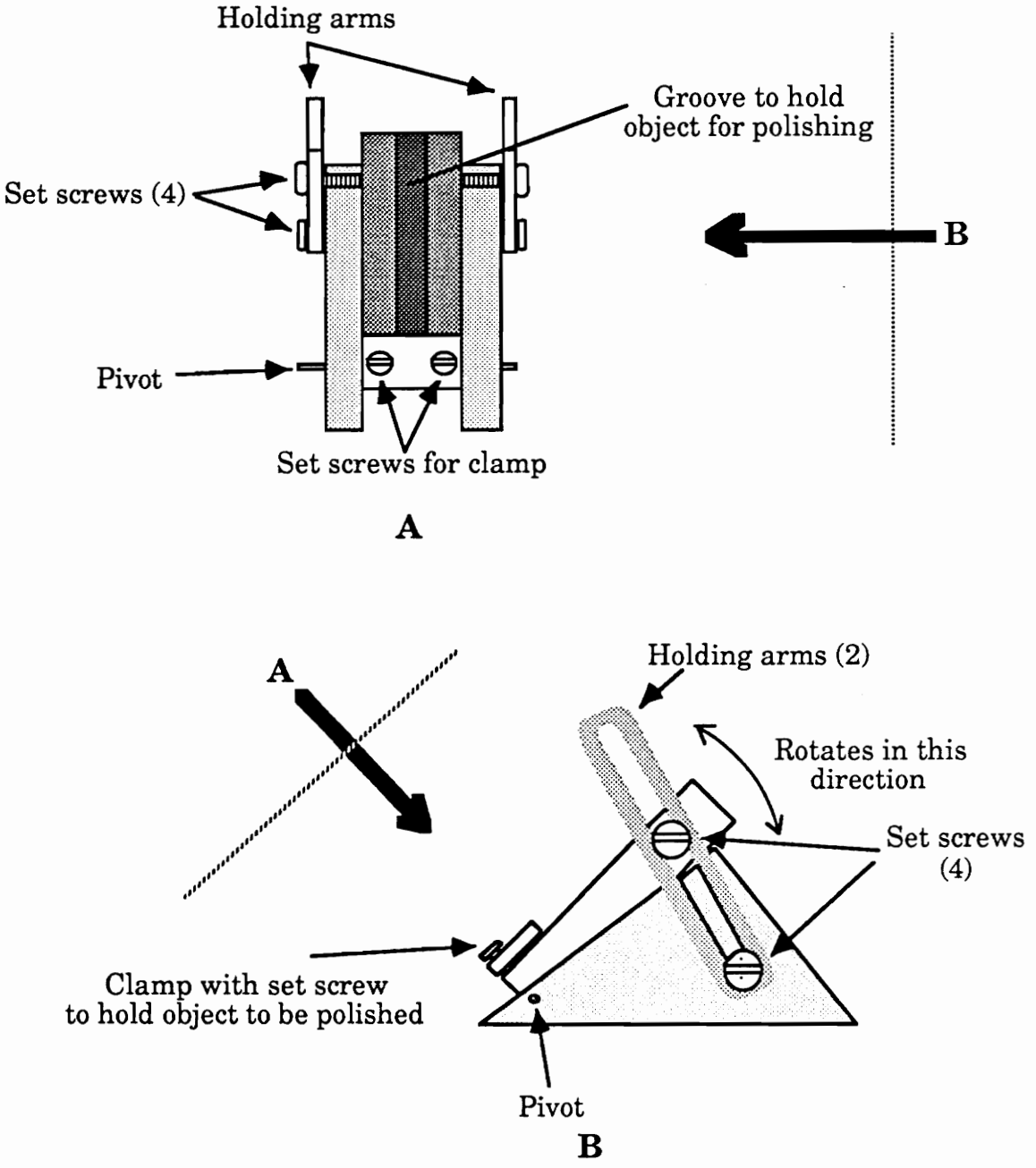

Figure 18. Schematic of the polishing jig used to polish the 45° angles for the beam-splitter.

Figure 19 shows the progression of the next two steps in the process. The first is to place a stripped region of the sensing fiber on two of the slides. The other two slides are placed on top of the first two as shown in the figure. A small, thin layer of epoxy is placed between the slides and cured. These two sets of slides and fiber are now permanent. The second part of Figure 19 shows the beam-splitter after the epoxy has cured. The fiber between the two sets of slides is then cleaved so that the end faces can be polished. The final plane of polish is also indicated in the figure. As can be seen, the planes of polish are designed in such a way that the finished pieces will realign properly.

After the slides are polished, they can be realigned using micropositioners. Figure 20 shows a closer view of the two halves of the splitter after polishing and realignment. The realignment process is done actively in order to monitor the power levels of the reflected and transmitted signals. During realignment, the final output fiber (after the splitter) and the input fiber (also e-core two-mode) are strained to ensure that changes in both fibers cause an oscillation at the output of the final fiber. If alignment is not precise, strain in the output fiber will cause oscillation, but strain in the input fiber will cause signal degradation. This is due to the two-mode nature of the fiber. The output fiber will be two-mode whether both modes from the sensing fiber transfer through or only part of these modes transfer. So, the alignment must ensure that both modes transmit through the splitter into the output fiber. If the alignment is off, only one mode will be transmitted and the splitter will not work.

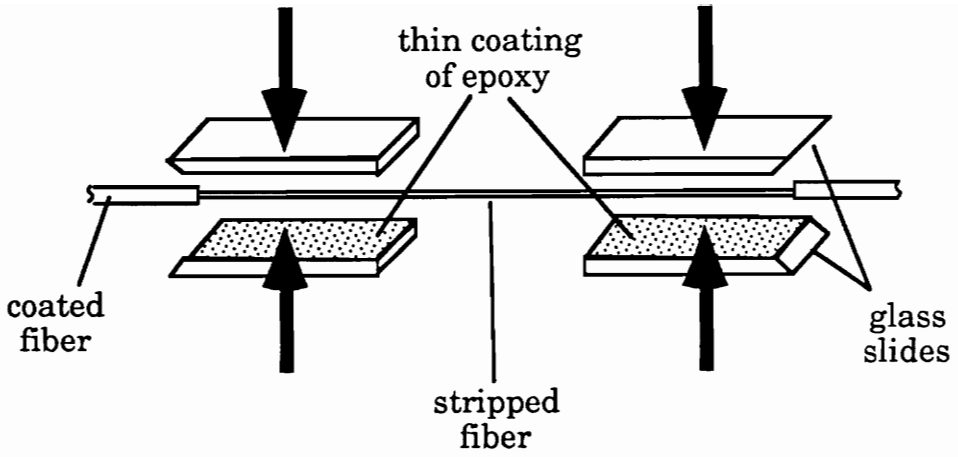

(a)

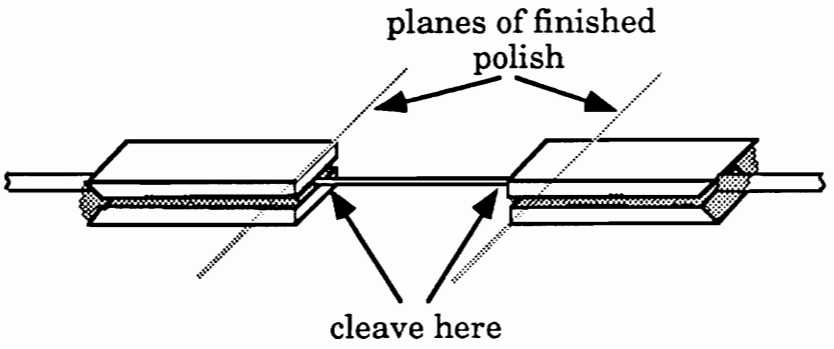

(b)

Figure 19. First two steps in the fabrication of the in-line beam splitter with (a) before the individual parts ar placed together and (b) after the epoxy has cured. Note that the shaded region represents the epoxy in both parts.

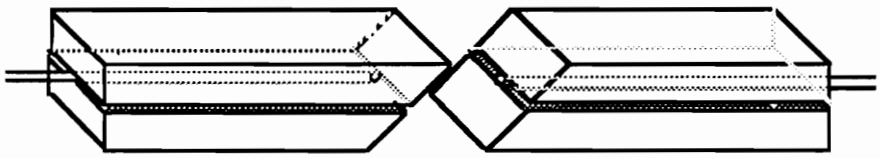

(a)

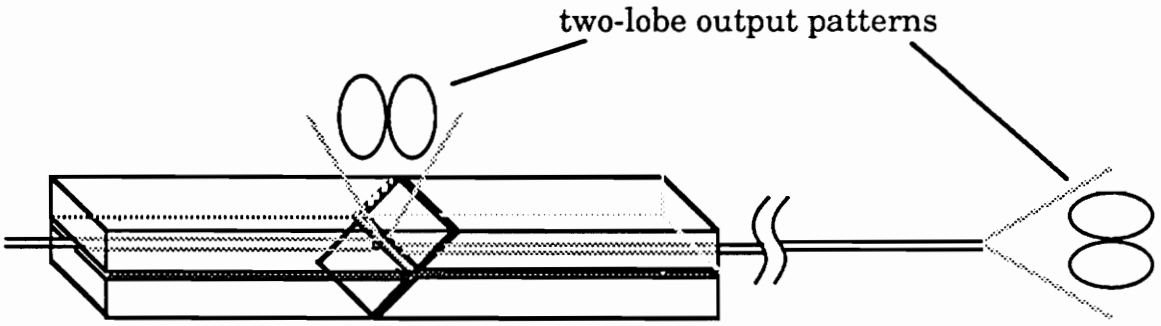

(b)

Figure 20. Closer view of beam-splitter after 45° angles are polished. (a) Before alignment. (b) After alignment.

4.2.3 Experiment and results

An experiment was designed to test the in-line beam-splitter. The setup for this experiment is shown in Figure 21. The entire length of fiber for this experiment is e-core two-mode fiber. Insensitive lead fibers are not necessary in this experiment because the splitter is being tested and the environment can be controlled to insure no perturbations affect the fiber except those desired. The first static strain controller is used to set the operating point of the sensing fiber which will give a known starting point for the strain. The PZT cylinder supplies the external perturbation to be measured by the sensor. The second static strain controller is used to set the phase difference between the two signals. As the strain on the output fiber is changed, the phase of its output with respect to the reflected signal will change. The desired phase difference, usually 90°, can be chosen.

As stated earlier, the realignment of the fiber ends is the most difficult part of the setup. Two cores with dimensions 1.25 x 2.5 μm polished at a 45° angle must be realigned. Obviously, misalignment of as little as 0.5 μm causes major changes in the modal coupling between the fibers. Since both modes must couple into the output fiber in relatively equal amounts, the alignment is critical. The alignment is performed with the power to the PZT turned off. First, the two halves are aligned for maximum power. Then the static strain controllers are used to change the strain on the input and output fibers. If the two-lobe pattern oscillates with strain in both of these fibers, it is properly aligned. In most cases, strain in the output fiber

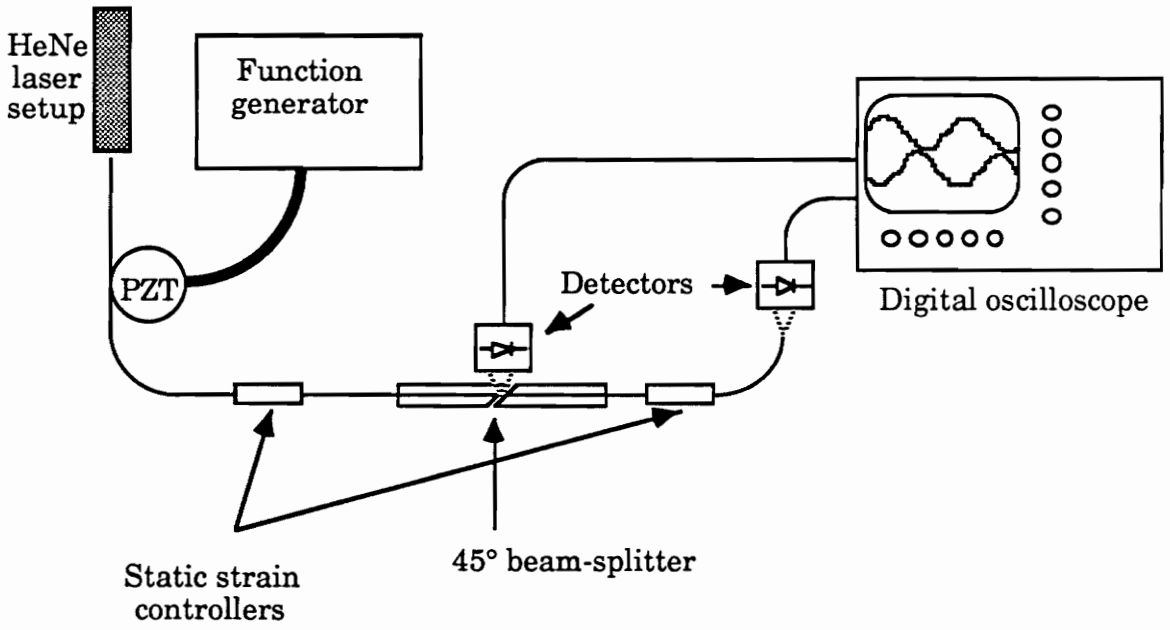

Figure 21. Experimental setup to test the in-line beam-splitter.

causes oscillation, but strain in the input fiber does not. When this occurs, the alignment is adjusted until strain in both fibers causes the proper oscillation. Alignment is then complete.

After completing the alignment of the beam-splitter, the power to the PZT is turned on. This causes a constant oscillating strain in the fiber. The amount of fiber wrapped around the PZT must be great enough to insure that fringing occurs. This is necessary to prove the phase changing capabilities of the splitter. The outputs of both detectors are displayed on the oscilloscope and the phase difference can be seen. By changing the static strain in the output fiber, this phase difference can be changed. Figures 22 through 24 show the ability to choose the phase difference between the two signals. Figure 22 shows the two signals in phase, before any adjustments have been made. Using the second static strain controller, the phase difference is changed to 90°, as seen in Figure 23. This phase difference can be changed to any desired value, such as 180° as seen in Figure 24. When looking at a larger portion of the signal, a period of oscillation for the PZT can be seen. This period includes regions corresponding to an increase in strain, a change of direction, and then a decrease of strain. As can be seen in Figure 25, the output signals from the detector exhibit a lead-lag quality. In other words, when strain is increasing, one signal is leading the other, and when strain is decreasing, this signal will be lagging. This therefore allows the determination of whether strain is increasing or decreasing, and fringe counting can be accomplished with the in-line beam-splitter.

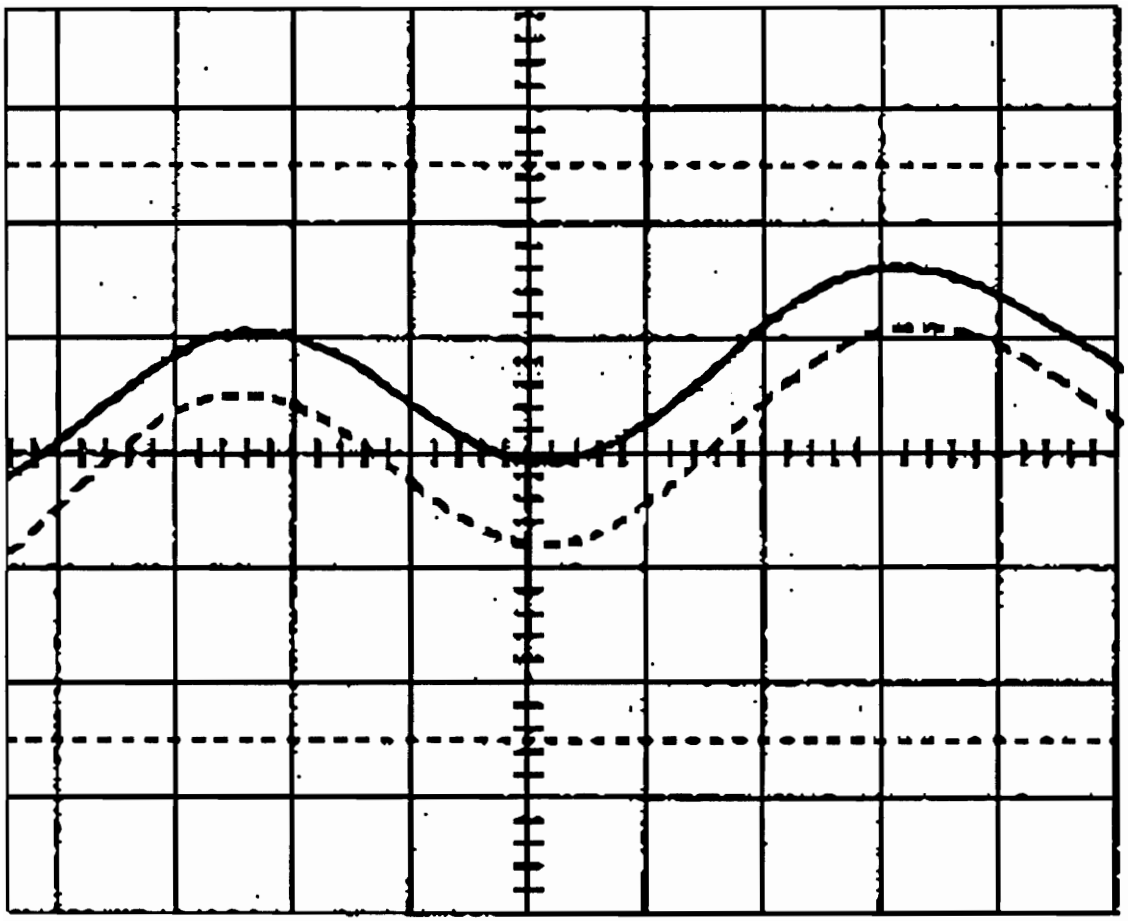

Figure 22. Oscilloscope trace of the two output signals in phase.

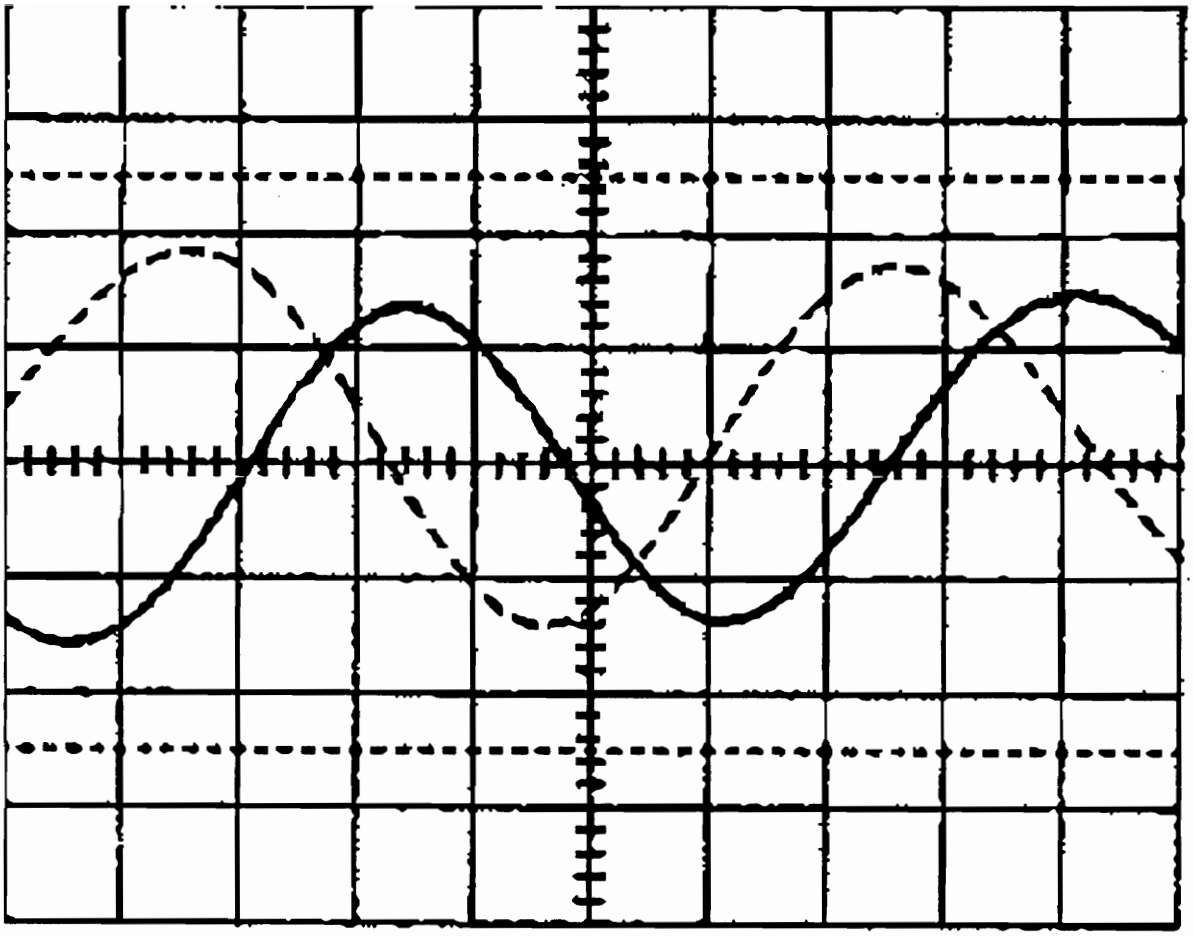

Figure 23. Oscilloscope trace of the two signals 90° out of phase.

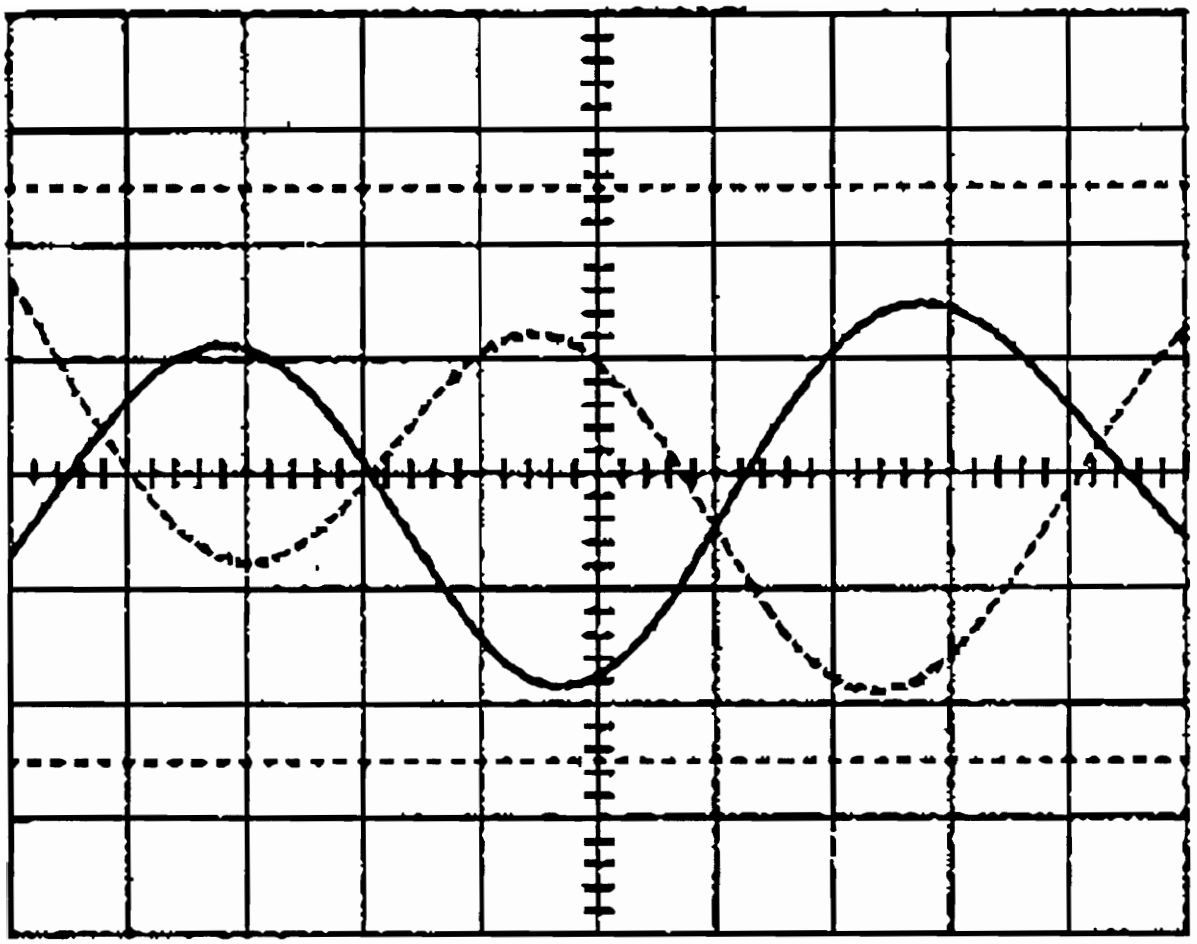

Figure 24. Oscilloscope trace of the two output signals approximately 180° out of phase.

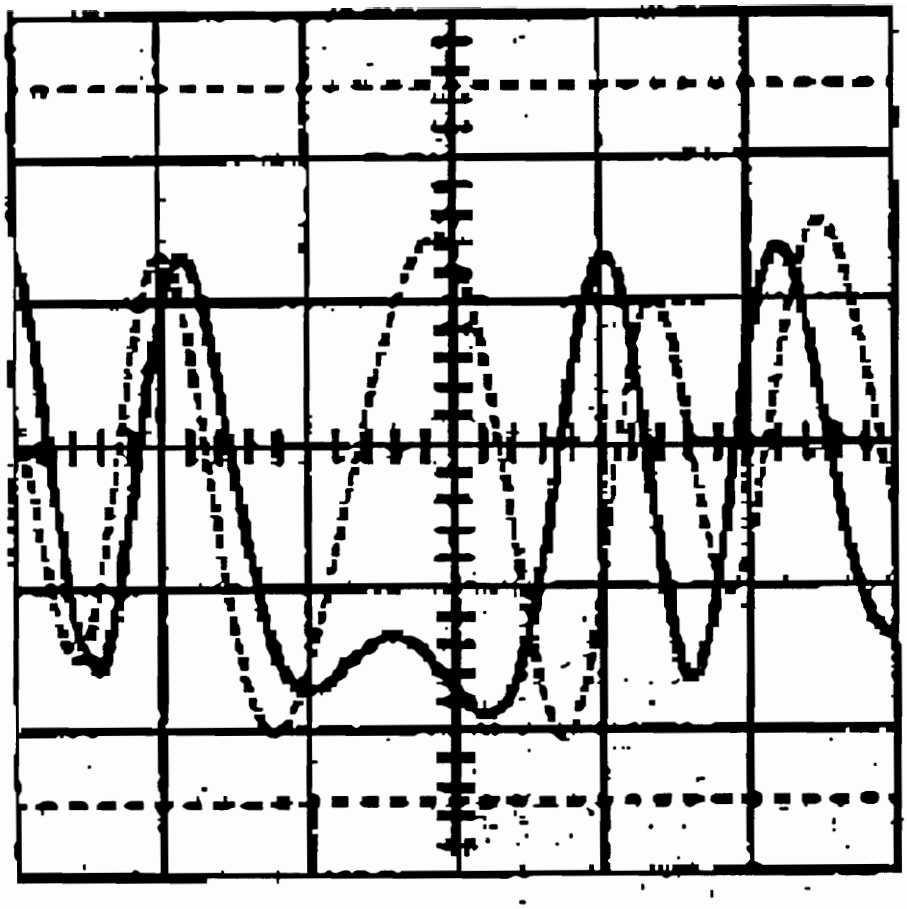

Figure 25. Oscilloscope trace showing lead-lag quality of the two outputs. The dashed curve leads the solid curve until the change from increasing strain to decreasing strain, nearly in the center of the trace. After this change, the dashed curve lags the solid curve.

4.3 Sensors Embedded in Composites

4.3.1 Experiment and results

An experiment was designed to compare the sensitivities of two fibers embedded between different laminae of a graphite-epoxy composite specimen. The composite was a regular cross-ply laminate consisting of laminae alternating between 0° and 90° with respect to the major dimension of the panel. The optical sensor fibers were placed between laminae 1 and 2 and between laminae 2 and 3. Figure 26 depicts the layup of the composite before cure, including the position of the fibers and the placement of the alternating layers. Note that the fibers were placed parallel to the major dimension of the panel, or parallel to the 0° graphite fibers in the composite. The assumption made for this experiment was that the optical fibers would move into the layers with parallel graphite fibers, the 0° layers, during the cure process. Figure 27 shows the composite after cure with the fibers placed in their predicted locations. This composite was then stressed and readings were taken for both sensors. These readings were then compared with predicted values using the estimated positions of the fibers in the composites after cure.

The experimental setup used to test these fibers is shown in Figure 28. The perturbation region is now the composite panel which is placed under load. For this test, a dynamic stress, or vibration, was used for the perturbation. The oscilloscope was used to retain the two signals representing the two

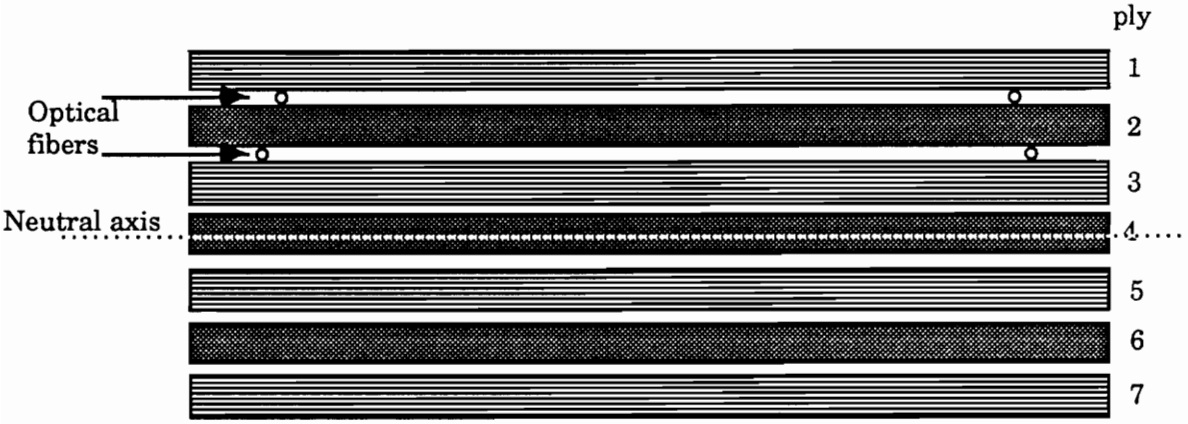

Figure 26. Schematic of composite layup before cure.

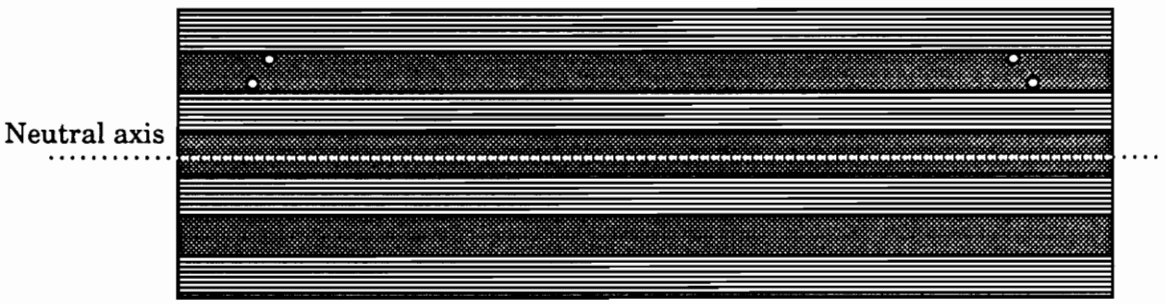

Graphite fibers parallel to the optical fiber (0°)

Graphite fibers perpendicular to the optical fiber (90°)

Figure 27. Schematic of predicted cross-section of composite after cure.

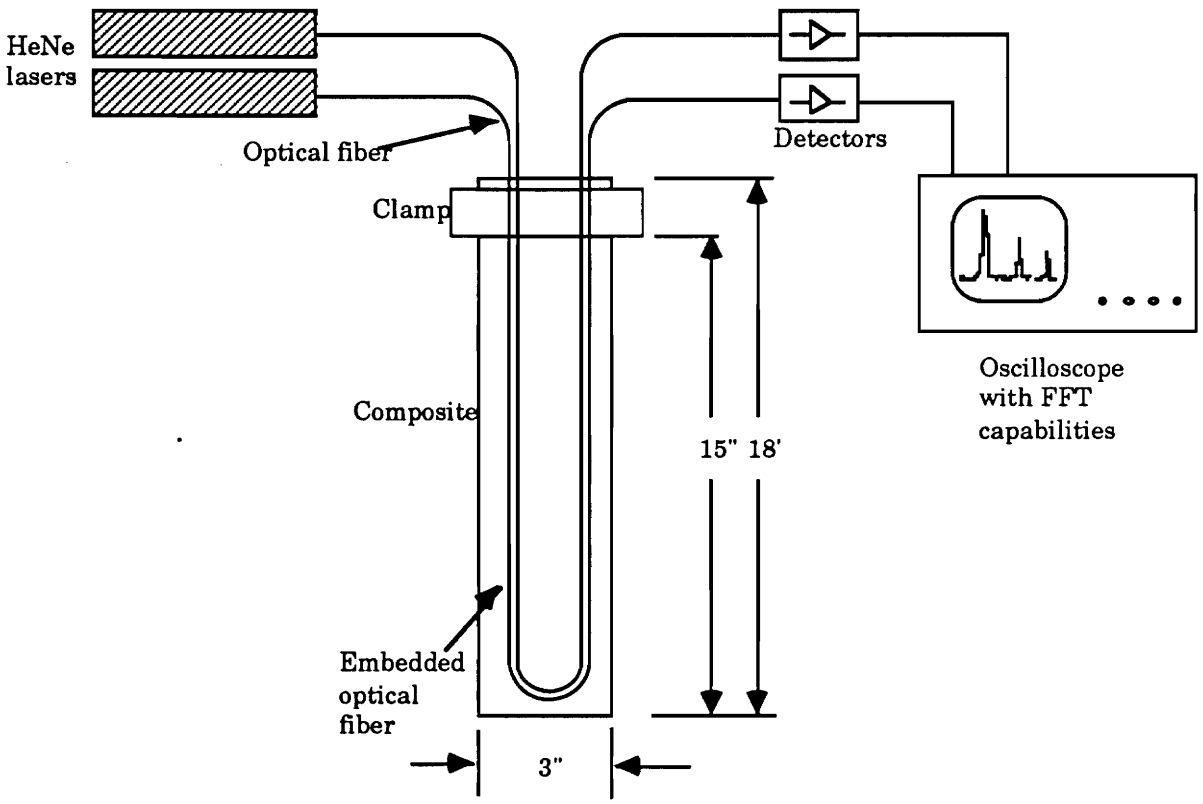

Figure 28. Experimental setup to test sensors embedded within the composite panel.

sensors. These signals were then compared at a specific location on the trace to determine the sensitivity comparison for the two sensors.

If we assume that the strain is transferred faithfully from the composite to the fiber, we can derive the deformation in the fiber due to a known tip displacement of the specimen, loaded in a cantilever beam geometry. This is given as

$$\Delta L = \frac{3\,\partial_y\, a}{2\,L}\ , \tag{4.3.1}$$

where L is the length of the composite, ∂_y is the tip displacement of the composite beam, and "a" is the distance of the fiber from the neutral axis. Appendix A gives the full derivation of this formula. Knowing that L and ∂_y are the same for both fibers in the composite, we can find the ratio between the deformations for the two sensors in terms of only their distances from the neutral axis. This ratio is given by the formula

$$\frac{\Delta L_1}{\Delta L_2} = \frac{a_1}{a_2}\,. \tag{4.3.2}$$

In equation (4.3.2), the subscripts 1 and 2 represent the outermost and innermost fibers, respectively. Using the value of 101.6 μm for $\Delta L_{2\pi}$ found in section 4.1.3, we have measured the ratio of the sensitivities for the two fibers to be 1.38. For a second test, the ratio was measured to be 1.44. These ratios were determined by translating the change in output power for one vibration to the corresponding strain necessary for that change in output power. The strains for the two fibers are then used for the ratio. The

calculated ratio of a_1/a_2 is 1.27 using typical values for the thickness of a laminae and the outer diameter of the fiber. The discrepancies in the calculated and measured results arise from the assumption that the lengths are the same for both fibers. In reality, the outermost fiber in the composite is slightly longer than the inner fiber due to the necessity that the fibers not cross over one another. The fibers should not cross one another because the pressure during cure could break one or both of the fibers. Therefore, the outer fiber is laid out in a pattern slightly larger than the inner fiber. Figure 28 showing the experimental setup shows this difference in length.

4.3.2 Discussion

As noted in the previous section, there were many assumptions made during the experiment. This section will discuss these assumptions and comment on their effect on the outcome of the experiment.

The major assumption made during the experiment was the final position of the fibers in the composite after the curing process. It was assumed that the fibers "moved" into the laminae with parallel graphite fibers, in this case the 0° laminae. This assumption was made because the pressure from the press and the relative inflexibility of the graphite fibers perpendicular to the optical fiber would tend to force the optical fiber away from the 90° laminae. The 0° laminae, however, will shift and move to allow the optical fiber to "move" into this laminae. To check on this

assumption, the composite was cut apart after the experiment and observed under a microscope. Figure 29 is a photomicrograph of one of the embedded optical fibers in the composite. It can be seen that the fiber does indeed move into the 0° layer. Figure 30 is a picture under less magnification showing the two fibers and their relative position in the composite. This picture also shows that the layers around the optical fiber are not affected by the presence of the optical fiber as long as one of the adjacent laminae has graphite fibers parallel to the optical fiber.

A second assumption was the thickness of each laminae of the composite. This value is actually an average value and the changes in thickness can be seen in Figure 30. If the thicknesses change randomly, although by small amounts, the strain in the sensor will change. This may also cause errors in the comparison of calculated and measured data. Other factors present in most fiber optic sensing schemes, such as laser drift, other external perturbations, and detector noise, were also ignored. Any of these could also cause small discrepancies between the measured and calculated values.

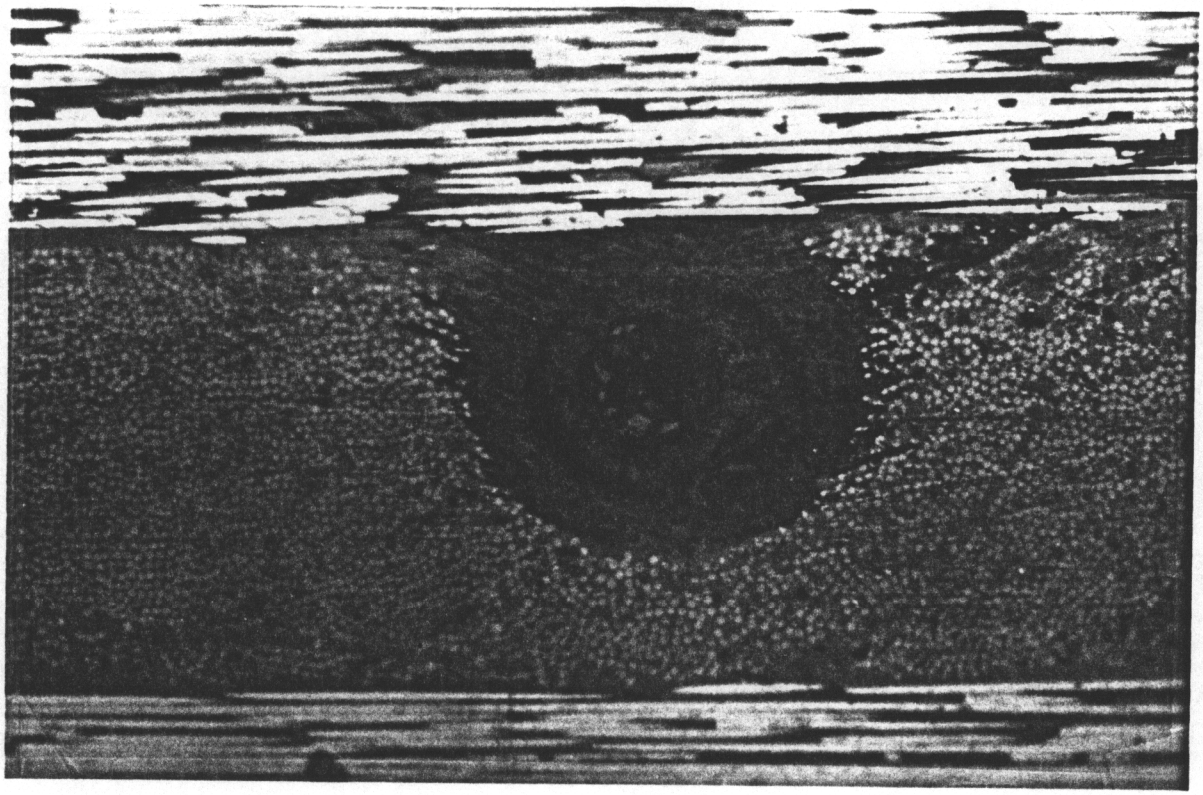

Figure 29. A photomicrograph of the cross section of a composite with an embedded optical fiber.

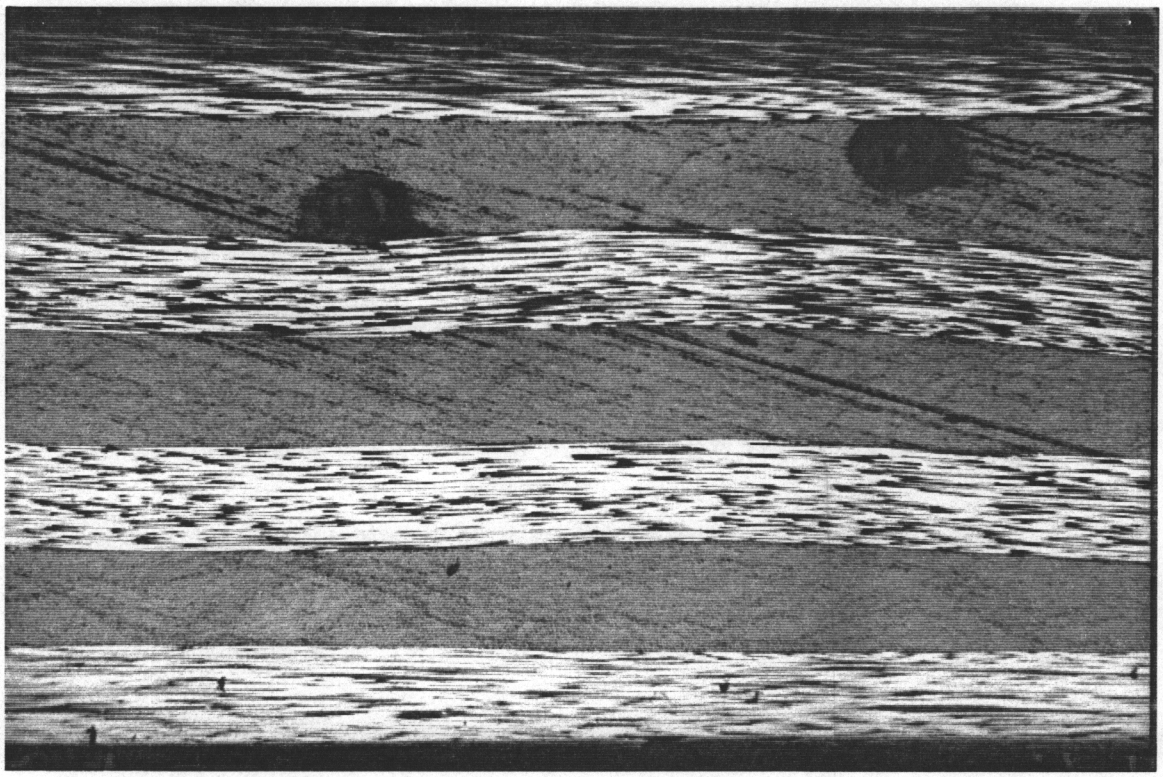

Figure 30. A photomicrograph of the cross section of the composite showing the relative position of the two embedded fibers.

5.0 Conclusion

This thesis has proven the practicality of the two-mode e-core sensor with insensitive leads and the use of an in-line beam-splitter to facilitate fringe counting. The fabrication of the insensitive lead sensor has been thoroughly described and the insensitivity of the leads demonstrated. The fabrication of the in-line beam-splitter has also been described and the ability to achieve two signals 90° out of phase has been demonstrated. The change in sensitivity of sensors embedded between different laminae of a composite has also been shown to be easily determined.

Future work for this sensor should include an exact theoretical analysis of the modes in the e-core fiber. As mentioned before, researchers at FEORC are deriving a numerical analysis of the modes in the e-core fiber. This derivation will allow a more precise and simpler method for the theoretical prediction of the outcome of experiments.

Future work for the insensitive lead fibers should include a more thorough study of the effects of embedding on the sensor. Work should also be done to

change the sensing length of the sensor to allow the detection of strain at a specific point in a composite. This will allow the possibility of placing many such sensors in a composite to give a map of the strain over the entire composite.

The electronics for fringe counting using the in-line beam-splitter are now being built. These electronics will allow both the counting of fringes and the determination of whether strain is increasing or decreasing by using the lead-lag quality of the beam-splitter. The possibility of attaching fibers to the beam-splitter should also be investigated. This will allow the placement of the splitter further from the electronics and decrease the need for a length of sensitive fiber from the sensing region to the splitter. The packaging of the splitter also needs to be investigated to make it more practical.

Appendix A

The theoretical derivation for the change in length (ΔL) of an optical fiber at a distance "a" from the neutral axis of a cantilever beam under a tip displacement ∂_y is presented. The distance "a" is measured from the neutral axis of the beam to the center of the optical fiber. Figure 31 is a schematic showing the values described in the derivation.

The change in length of the fiber is represented as the integral of the strain at each point on the beam over the length of the beam and is given by[34]

$$\Delta L = \int_0^L \varepsilon_x \, dx \,, \tag{A.1}$$

where ε_x is the strain at each point and L is the length of the beam. The strain at each point on the beam can be represented by[34]

$$\varepsilon_x = \frac{P\,(L - x)\,a}{E\,I} \,, \tag{A.2}$$

where P is the applied force, E is Young's modulus for the beam, and I is the moment of inertia for the beam. The tip diaplacement of the cantilever beam is given by

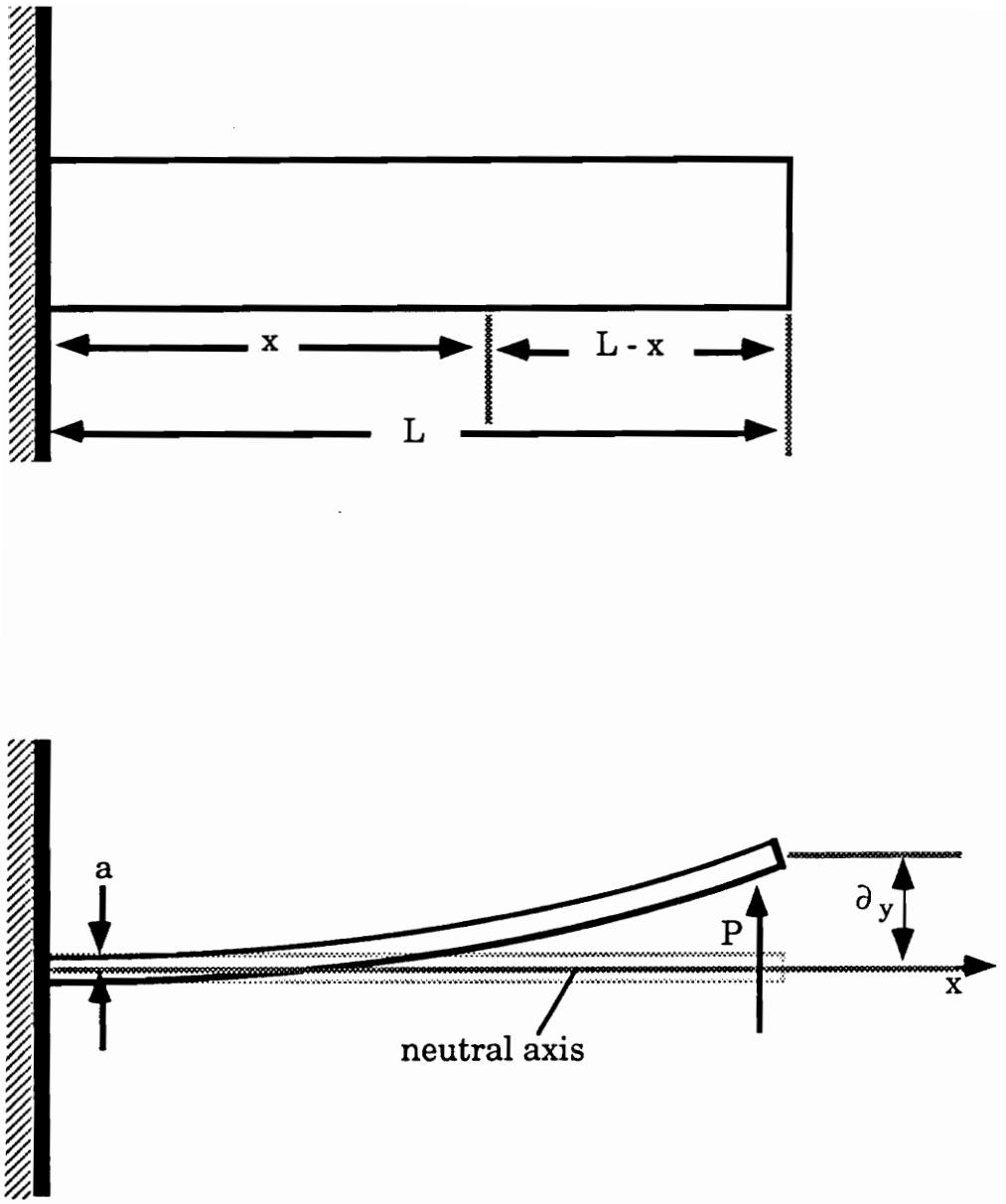

Figure 31. Schematic of tip displacement for a cantilever beam.

$$\partial_y = \frac{P L^3}{3 E I}. \qquad (A.3)$$

This equation can be manipulated to give

$$E I = \frac{P L^3}{3 \partial_y}. \qquad (A.4)$$

Substituting the above result for EI into equation (A.2) the change in length for the optical fiber is given by

$$\Delta L = \frac{3 \partial_y a}{L^3} \int_0^L (L - x)\, dx . \qquad (A.5)$$

Solving the integral and substituting in the limits of integration, the final solution for the change in length of the optical fiber is given by

$$\Delta L = \frac{3 \partial_y a}{2 L} , \qquad (A.6)$$

which is the same as equation (4.3.1).

References

1. R. O. Claus, A. Safaai-Jazi, K. D. Bennett, R. G. May, B. D. Duncan, and A. M. Vengsarkar, "Smart structures research program at Virginia Tech," Proc. SPIE O/E Fiber Lase, (Boston MA), September 1988.

2. E. Udd, "Overview of fiber optic smart structures for aerospace applications," Proc. SPIE O/E Fiber Lase, (Boston MA), September 1988.

3. R. S. Rogowski, "Smart structures for NASA missions," Proc. SPIE O/E Fiber Lase, (Boston MA), September 1988.

4. R. O. Claus and J. H. Cantrell, "Detection of ultrasonic waves in solids by an optical fiber interferometer," Proc. IEEE Ultrasonics Symposium, (Boston MA), p.719, October 1980.

5. R. O. Claus, K. D. Bennett, A. M. Vengsarkar, and K. A. Murphy, "Embedded optical fiber sensors for materials evaluation," Journal of Nondestructive Evaluation, Vol. 8, No. 2, p.371, 1989.

6. R. M. Jones, Mechanics of Composite Materials, Scripta Book Co., 1975.

7. B. D. Duncan, Modal Interference Techniques for Strain Detection in Few-Mode Optical Fibers, M. S. Thesis, VPI&SU, April 1988.

8. P. A. Ehrenfeuchter, Modal Domain Detection of Vibration in Beams, M. S. Thesis, VPI&SU, December 1986.

9. B. Y. Kim, "Few mode fiber devices," OSA Optical Fiber Sensors Conference, New Orleans, Louisiana, 1988.

10. B. Y. Kim, J. N. Blake, S. Y. Huang, H. J. Shaw, "Use of highly elliptical core fibers for two-mode fiber devices," Applied Optics, Vol. 12, p.729, 1987.

11. M. R. Layton and J. A. Bucaro, "Optical fiber acoustic sensor utilizing mode-mode interference," Applied Optics, Vol. 18, p.666, 1979.

12. L. G. Cohen, W. G. French, and C. Lin, "Propagation characteristics of double-mode fibers," Technical Digest of Topical Meeting on Optical Fibre Communications, Washington, p.98, 1979.

13. N. Shibata, M. Tateda, S. Seikai, and N. Uchida, "Spatial technique for measuring modal delay differences in a dual-mode optical fibre," Applied Optics, Vol. 19, p. 1489, 1980.

14. L. G. Cohen, W. L. Mammel, C. Lin, and W. G. French, "Propagation characteristicsof double-mode fibres," Bell System Technical Journal, Vol. 59, p. 1061, 1980.

15. J. L. McMillan, "Novel technique for measurement of wavelength of zero relative delay between modes of a dual-mode optical fibre," Electronics Letters, Vol. 18, p. 240, 1982.

16. P. D. Nichols, "Comparison between techniques for measuring the LP_{11}-mode cutoff wavelength in monomode fiber," Electronics Letters, Vol. 18, p. 1008, 1982.

17. J. L. McMillan and S. C. Robertson, "Dual-mode optical-fibre interferometric sensor," Electronics Letters, Vol. 20, p. 136, 1984.

18. R. C. Youngquist, J. L. Brooks, and H. J. Shaw, "Two-mode fiber modal coupler," Optics Letters, Vol. 9, p. 177, 1984.

19. W. V. Sorin, B. Y. Kim, and H. J. Shaw, "Phase-velocity measurements using prism output coupling for single- and few-mode optical fibers," Optics Letters, Vol. 11, p. 106, 1986.

20. W. V. Sorin, B. Y. Kim, and H. J. Shaw, "Highly selective evanescent modal filter for two-mode optical fiber," Optics Letters, Vol. 11, p. 581, 1986.

21. N. K. Shankaranarayanan, Mode-Mode Interference in Optical Fibers: Analysis and Experiment, M. S. Thesis, VPI&SU, March 1987.

22. N. K. Shankaranarayanan, K. T. Srinivas, and R. O. Claus, "Mode-mode interference effects in axially strained few-mode optical fibers," Proc. SPIE O/E Fiber Lase, August 1987.

23. A. Safaai-Jazi and R. O. Claus, "Synthesis of interference patterns in few-mode optical fibers," Proc. SPIE O/E Fiber Lase, (Boston MA), 1988.

24. J. N. Blake, S. Y. Huang, B. Y. Kim, and H. J. Shaw, "Strain effects on highly elliptical core two-mode fibers," Optics Letters, Vol. 12, p. 732, 1987.

25. S. Y. Huang, J. N. Blake, and B. Y. Kim, "Perturbation effects on mode propagation in highly elliptical core two-mode fibers," Journal of Lightwave Technology, Vol. 8, p. 23, 1990.

26. C. Yeh, "Elliptical Dielectric waveguides," Journal of Applied Physics, Vol. 33, p. 3235, 1962.

27. P. D. Gianino, B. Bendow, and P. Wintersteiner, "Propagation characteristics of irregularly shaped step-index fiberguides," Advances in Ceramics, vol. 2, Physics of Fiber Optics, Editors B. Bendow and S. Mitra, The American Ceramic Society Inc., p. 330.

28. L. Eyges, P. Gianino, and P. Wintersteiner, "Modes of dielectric waveguides of arbitrary cross sectional shape," Journal of the Optical Society of America, Vol. 69, p. 1226, 1979.

29. A. W. Snyder and X. H. Zheng, "Optical fibers of arbitrary cross sections," Journal of the Optical Society of America A, Vol. 3, p. 601, 1986.

30. A. Kumar and R. K. Varshney, "Propagation characteristics of dual-mode elliptical-core optical fibers," Optics Letters, Vol. 14, p. 817, 1989.

31. K. Shaw and A. M. Vengsarkar, "Numerical analysis of elliptical-core optical fiber waveguides," Internal report, Fiber & Electro-Optics Research Center, VPI&SU, 1990.

32. K. A. Murphy, M. S. Miller, A. M. Vengsarkar, R. O. Claus, and N. E. Lewis, "Embedded modal domain sensors using elliptical-core optical fibers," Proc. SPIE O/E Fiber Lase, (Boston MA), September 1989.

33. J. N. Blake, S. Y. Huang, and B. Y. Kim, "Elliptical core two-mode fiber strain-guage," Proc. SPIE O/E Fiber Lase, August 1987.

34. F. P. Beer and E. R. Johnston, Mechanics of Materials, McGraw-Hill Inc., 1981.

VITA

Mark S. Miller was born on November 29, 1966 in Rochester, New York. He graduated from Gates-Chili High School, Rochester, New York, in 1984. He received a Bachelor of Science degree in Electrical Engineering from Virginia Polytechnic Institute and State University in November, 1987. His research interests include fiber optic devices and sensors.

Mr. Miller is a member of the IEEE Communications Society and the Optical Society of America.